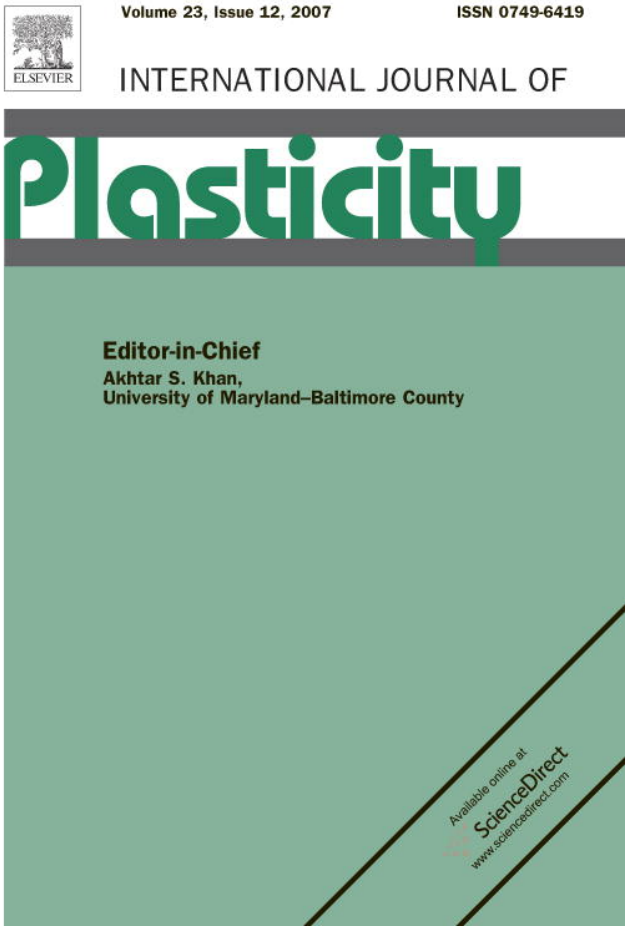

Available online at www.sciencedirect.com
ScienceDirect
International Journal of Plasticity 23 (2007) 2085–2114
INTERNATIONAL JOURNAL OF Plasticity
www.elsevier.com/locate/ijplas

A simple theory of strain gradient plasticity based on stress-induced anisotropy of defect diffusion

K.Y. Volokh *, P. Trapper

Faculty of Civil and Environmental Engineering, Technion – Israel Institute of Technology, Haifa 32000, Israel

Received 12 December 2006; received in final revised form 7 February 2007
Available online 2 March 2007

Abstract

A new strain gradient plasticity theory is formulated to accommodate more than one material length parameter. The theory is an extension of the classical J_2 flow theory of metal plasticity to the micron scale. Distinctive features of the proposed theory as compared to other existing theories are the simplicities of mathematical formulation, numerical implementation and physical interpretation.

The proposed theory is based on the physical idea that the effective plastic strain is a measure of the defect[1] density. The latter allows interpreting the yield/hardening condition as an equation describing (quasi-static) evolution of defects. At the macroscopic scale, the defect diffusion is negligible and the yield condition is a purely algebraic equation. At the scale of microns, however, the defect diffusion is sound and it can be included in the yield condition through the divergence of the vector of the defect flux. We propose that the defect flux is linearly proportional to the gradient of the defect density, i.e. the accumulated plastic strain. This proportionality is provided by a second-order tensor of the *defect conductivity*. Such tensor is the main source of the material characteristic lengths. If, for example, this tensor is equivalent to the length-scaled identity tensor then we arrive at the earlier Aifantis theory of strain gradient plasticity where the defect diffusion is isotropic. It is reasonable, however, to assume that the defect diffusion is not purely isotropic and stresses induce anisotropy. The latter means that the defect conductivity tensor should depend on the scaled stress tensor. The corresponding formulation of strain gradient plasticity is developed in the present work. It appears that the proposed theory is, probably, the simplest one among the theories, which include

* Corresponding author.
E-mail address: cvolokh@tx.technion.ac.il (K.Y. Volokh).

[1] Point, line (dislocations), and surface defects underlying plastic flow are considered. These defects should not be confused with microcracks, voids etc underlying damage accumulation. The latter is out of the scope of the present work.

0749-6419/$ - see front matter
doi:10.1016/j.ijplas.2007.02.006

more than one characteristic length. It is also important that in contrast to the majority of strain gradient theories no direct use of higher-order stresses, which can hardly be interpreted in simple physical terms, has been made in the present work.

Keywords: Defects/dislocations; Plasticity theory; Strain gradients

1. Introduction

Over the past few decades the research focus in materials science and solid mechanics has shifted towards small length scales. This trend was necessitated by the technological development of small structures like MEMS, thin films, etc. on the one hand and the need to understand and hopefully design materials based on their microstructural properties on the other hand. Traditional approaches of the classical continuum mechanics fail to provide vital information about mechanical behavior of materials and structures at the micron scale. For example, experiments with wire torsion and film bending as well as the indentation tests unambiguously demonstrate that inelastic deformation of metal structures is size-dependent at the micron scale: smaller is stronger (e.g. Fleck et al., 1994; Fleck and Hutchinson, 1997; Nix and Gao, 1998; Stolken and Evans, 1998; McElhaney et al., 1998; Hutchinson, 2000). Evidently, the classical formulation of continuum mechanics, which is length-independent, should be modified to display the size effect.

An implicit and physically sound (yet computationally involved) way to account for the size effect is to consider the dynamics of defects/dislocations (Devincre and Kubin, 1997; Zbib et al., 2002; Deshpande et al., 2005; Ohashi et al., 2007). An explicit and phenomenological way to account for the size effect is to consider enhanced continuum formulations where the characteristic length appears naturally in the governing equations. It is possible, for example, to introduce non-local continua where the stress at a point depends on the deformation history in finite and small neighborhood of the considered point. The size of this neighborhood is the desired length scale. Such an approach is based on an integral rather than a differential dependence in the constitutive equations (Bazant et al., 1984; Pijaudier-Cabot and Bazant, 1987). This approach has mainly been employed in conjunction with a damage theory formulation but can also be used to introduce a length scale into a plasticity theory (Leblond et al., 1994; Stromberg and Ristinmaa, 1996; Needleman and Tvergaard, 1998; Polizzotto et al., 1998; di Luzio and Bazant, 2005). Another approach to the enhancement of the classical continuum is provided by relaxing the assumption that the stress at a point depends on the first gradient of deformation only. The introduction of the second deformation gradient leads to a variety of the 'gradient' theories which present the mainstream of the works on the length-dependent elastic–plastic continua. The name 'gradient' reflects the idea of introducing the characteristic lengths as scaling factors for the spatial derivatives of strains (second gradients of deformations) in order to provide the dimensional consistency of differential equations. Aifantis (1984) introduced this idea in his pioneering work on strain gradient plasticity (SGP) where a length-scaled Laplacian of the effective plastic strain was included in the yield condition. This formulation acquired a sound mathematical form in the work by Muhlhaus and Aifantis (1991) and led to the growing interest in the development of various SGP theories (de Borst, 1993).

Among the influential developments of SGP we mention a series of papers by Fleck et al. (1994) and Fleck and Hutchinson (1993, 1997, 2001). The earlier papers of these authors introduced a phenomenological SGP as an extension of the Toupin–Mindlin elasticity theory (with higher-order stresses work-conjugate to spatial derivatives of strains) to inelasticity. Later Fleck and Hutchinson (2001) reformulated their earlier higher-order SGP theory aiming at the significant reduction of the number of unknowns and equations. Such compactification allowed them to introduce three independent length factors within a relatively simple theoretical framework. A variety of theories have been developed aimed at relating the parameters that enter a phenomenological theory to physical quantities. Many of them focus on crystalline solids where the deformation mechanism is dislocation glide. For example, Gao et al. (1999) and Huang et al. (2000) introduced a phenomenological SGP where a multi-scale link to the microscopic dislocation structure had been made. Their approach has been further extended from phenomenological to crystal plasticity (Han et al., 2005a,b). Gurtin (2000, 2002, 2003) and Gurtin and Anand (2005) developed a very general and elegant size-dependent crystal plasticity framework. In a different context, a similar approach can be found in Gudmundson (2004) and Fredriksson and Gudmundson (2005). A variant of the physically based theory of gradient plasticity has been proposed by Al-Rub and Voyiadjis (2006) recently.

Reviewing the SGP development, we should mention that Acharya and Bassani (2000) and Bassani (2001) proposed a class of lower-order gradient theories, which main premise is that the higher-order gradients of plastic strains can be introduced in the tangent hardening moduli without adding boundary conditions (see also Huang et al., 2004; Liu et al., 2004; Hwang et al., 2004; Qu et al., 2006; Wallin and Ristinmaaw, 2005; Brinckmann et al., 2006; Zhang et al., 2007). Evidently, this premise is mathematically doubtful because the increase of the order of differential equations, as a result of the introduction of the higher-order gradients of plastic strains, should be accompanied by the introduction of additional boundary conditions, which provide the well-posedness of the boundary value problem. Advancing this argument Volokh and Hutchinson (2002) demonstrated that the problem of simple shear of an elastic–plastic layer is ill-posed within the framework of a lower-order SGP. Particularly, they showed that a third-order differential equation with only two boundary conditions prescribed by the lower-order SGP in the case of simple shear possesses an unlimited number of solutions, which can be readily generated numerically. Defending the lower-order SGP Acharya et al. (2004) presented a lengthy argument that, in our opinion, did not resolve the main problem of the lower-order theories – mathematical inconsistency. Unfortunately, this inconsistency is often hidden by numerical procedures that regularize the ill-posed problem implicitly. An interesting investigation of the validity of the lower-order theories can be found in Yun et al. (2004) where the principal conclusion directly supports the Volokh and Hutchinson's (2002) argument though on the different theoretical grounds. This point is further discussed in Huang et al. (2004) where the inability of the lower-order theories to capture the boundary layer solutions is emphasized.

In the present work, we develop a simple version of the phenomenological SGP theory naturally accommodating two (or more) characteristic lengths. The physical idea behind this development is that the accumulated effective plastic strain is a measure of defect/dislocation density (Aifantis, 1987). This allows interpreting the yield condition as a defect (quasi-static) evolution equation, which links the plastic hardening to the motion of defects. At the macroscopic scale, the defect diffusion is negligible and the

yield condition is a purely algebraic equation. At the scale of microns, however, the defect diffusion is sound and it can be included in the yield condition through the divergence of the vector of *defect flux*. We propose that the defect flux is linearly proportional to the gradient of the defect density, i.e. the accumulated plastic strain. This proportionality is provided by the introduction of a second-order tensor of the *defect conductivity*. Such tensor is the main source of the material characteristic lengths. If, for example, this tensor is equivalent to the length-scaled identity tensor then we arrive at the earlier Aifantis theory of strain gradient plasticity where the defect diffusion is isotropic. We assume, however, that the defect diffusion is not purely isotropic and stresses induce the diffusion anisotropy. The latter means that the scaled stress tensor should be a part of the defect conductivity tensor. The corresponding formulation of strain gradient plasticity is developed in the present work. It appears that the proposed theory is, probably, the simplest one among the theories, which include more than one characteristic length. It is also important that in contrast to the majority of strain gradient theories no direct use of higher-order stresses, which can hardly be interpreted in simple physical terms, has been made in the present work.

2. Governing equations

We consider equilibrium of elastic–plastic solids under small deformations

$$\operatorname{div}\boldsymbol{\sigma} = \mathbf{0} \quad \text{in } \Omega, \tag{1}$$

$$\boldsymbol{\sigma}\mathbf{n} = \bar{\mathbf{t}} \quad \text{or} \quad \mathbf{u} = \bar{\mathbf{u}} \quad \text{on } \partial\Omega, \tag{2}$$

where $\boldsymbol{\sigma}$ is the Cauchy stress tensor; $\mathbf{t}$ is a surface traction; $\mathbf{n}$ is a unit outward normal to the boundary $\partial\Omega$ of body Ω; and $\mathbf{u}$ is a displacement field. The barred quantities are prescribed.

The strain tensor is decomposed in the elastic and plastic parts

$$\boldsymbol{\varepsilon} = (\nabla\mathbf{u} + \nabla\mathbf{u}^{\mathrm{T}})/2 = \boldsymbol{\varepsilon}^{\mathrm{e}} + \boldsymbol{\varepsilon}^{\mathrm{p}}, \tag{3}$$

where the plastic deformation is incompressible

$$\operatorname{tr}\boldsymbol{\varepsilon}^{\mathrm{p}} = 0. \tag{4}$$

Hooke's law for isotropic elasticity takes the form

$$\boldsymbol{\sigma} = \mathbf{C} : (\boldsymbol{\varepsilon} - \boldsymbol{\varepsilon}^{\mathrm{p}}), \quad C_{ijmn} = (K - 2G/3)\delta_{ij}\delta_{mn} + G(\delta_{im}\delta_{jn} + \delta_{in}\delta_{jm}), \tag{5}$$

where K and G are the bulk and shear moduli accordingly.

The flow rule takes the form

$$\dot{\boldsymbol{\varepsilon}}^{\mathrm{p}} = \dot{\varepsilon}_{\mathrm{p}}\mathbf{m}, \tag{6}$$

where

$$\dot{\varepsilon}_{\mathrm{p}} = \sqrt{2\dot{\boldsymbol{\varepsilon}}^{\mathrm{p}} : \dot{\boldsymbol{\varepsilon}}^{\mathrm{p}}/3}, \tag{7}$$

$$\mathbf{m} = 3\mathbf{s}/(2\sigma), \tag{8}$$

$$\mathbf{s} = \boldsymbol{\sigma} - (\operatorname{tr}\boldsymbol{\sigma})\mathbf{1}/3, \tag{9}$$

$$\sigma = \sqrt{3\mathbf{s} : \mathbf{s}/2}. \tag{10}$$

Introducing the effective or accumulated plastic strain

$$\varepsilon_{\mathrm{p}} = \int \dot{\varepsilon}_{\mathrm{p}}\, \mathrm{d}t, \tag{11}$$

we can write the yield condition in the following form

$$f = \sigma - \sigma_y(\varepsilon_{\mathrm{p}}) - \mathrm{div}\mathbf{g}(\nabla\varepsilon_{\mathrm{p}}) = 0, \tag{12}$$

where the hardening function $\sigma_y(\varepsilon_{\mathrm{p}})$ is derived experimentally and $\mathbf{g}$ is a vector of the defect flux discussed below.

We have to comment on the physical phenomena underlying the phenomenological theory of plasticity in order to motivate the specific form of (12). We start with the notion, which is widely accepted by researchers in the field of metal plasticity, that the macroscopic plastic flow is essentially a result of the motion and accumulation of crystal defects[2] including point defects, dislocations, and surface defects. While the microscopic flow of the defects is usually confined to certain directions within the grains, the macroscopic plastic flow is an average over numerous grains and its direction is defined by the macroscopic (normalized) stress as it appears, for example, in the flow rule (6). The rate of the flow is defined by the rate of the accumulation of plastic strain – the plastic multiplier in (6). The flow rule cannot capture, however, the conditions of the flow onset. Such a condition – the yield condition – is usually separated from the flow rule and it depends on the current state of the defect distribution. The yield condition generally changes with the defect flow representing the so-called hardening effect. To characterize the state of the defect distribution its measure should be chosen. The defect density seems to be an appropriate measure of the microscopic defect distribution and it is natural to regard the accumulated plastic strain (11) as a macroscopic measure of the defect density. Thus, the yield condition depends on the accumulated plastic strain or the defect density. We interpret the yield condition as an indicator of the quasi-static evolution of the defect distribution. Such an indicator is usually set in the stress space. The latter, apparently, gave rise to the interpretation of the yield condition as the microforce balance by some authors. Such an interpretation is meaningless, of course, if the yield condition is set in the strain space. The latter is the reason why we prefer to consider the yield condition as an indicator of the evolution of the defect distribution without directly referring to its specific appearance. It is traditionally assumed that the yield condition depends only on the magnitude of the accumulated strain or the defect distribution and not on its spatial gradient. This assumption is natural because it allows ruling out non-local effects and preserving the length-independence of the macroscopic theories. If, however, the length-dependence is necessary as in the case of the structures at the micron scale or the problems of the shear band formation then the non-local nature of the defect distribution should be taken into account and the spatial gradients of the accumulated strain/defect density should be included in the yield condition. The latter can be arranged in a variety of ways. Keeping in mind that the yield condition describes the gradual evolution of the defect distribution, it is natural to set the yield condition in the form of a quasi-static evolution equation of the reaction diffusion type. Such a formulation implies the appearance of the third term on the right-hand side of (12) where a measure, $\mathbf{g}$, of the defect/accumulated strain flux is introduced. This measure is a function of the spatial gradient of the defect density/accumulated strain. Assuming the

[2] Of course, twinning, void growth, grain boundary sliding and phase transitions can also contribute to the plastic flow.

simplest linear relationship between the measure of the defect flux and the spatial gradient of the defect density we can write the following constitutive law

$$\mathbf{g} = -\mathbf{D}\nabla\varepsilon_{\mathrm{p}}, \tag{13}$$

where $\mathbf{D}$ can be called the *defect conductivity tensor* by analogy with similar laws in mass and heat transfer. It is reasonable to assume that the defect diffusion should be stress-dependent as the defect flow itself. Thus, the coefficient tensor $\mathbf{D}$ should be stress-dependent. Since we do not have enough information on this tensor, we can try the following formal way to make it more specific. First, we assume that $\mathbf{D}$ is approximated by a polynomial of the stress tensor

$$\mathbf{D}(\mathbf{m}) = a_1(I_2(\mathbf{m}), I_3(\mathbf{m}))\mathbf{1} + a_2(I_2(\mathbf{m}), I_3(\mathbf{m}))\mathbf{m} + a_3(I_2(\mathbf{m}), I_3(\mathbf{m}))\mathbf{m}^2, \tag{14}$$

where a_1, a_2, and a_3 are functions of the second I_2 and the third I_3 principal invariants of the normalized deviatoric stress tensor $\mathbf{m}$; and $\mathbf{1}$ is the second-order identity tensor. The first principal invariant equals zero $I_1 = 0$ by definition of $\mathbf{m}$. The higher-order terms in $\mathbf{m}$ can be reduced to the above form because of the Cayley–Hamilton theorem. Evidently, (14) can also be interpreted as a power series expansion of the unknown tensor function. Again, we do not know the specific forms of functions a_1, a_2, a_3 and we assume that they can be expanded in the power series with respect to the principal invariants of $\mathbf{m}$ or approximated by the polynomials of the invariants. Because of the lack of information we ignore all terms in such representations except constants

$$a_1 = b_1 = \text{constant}, \quad a_2 = b_2 = \text{constant}, \quad a_3 = b_3 = \text{constant}. \tag{15}$$

These constants are related to the characteristic lengths. We further reduce the number of constants to two

$$b_1 = E\alpha_1^2, \quad b_2 = -E\alpha_2^2, \tag{16}$$

where E is the elasticity modulus and α_1 and α_2 are the characteristic lengths. Negative sign is chosen for b_2 based on the solution of the void growth and beam bending problems, which are considered in Section 3. The negative sign prevents from the degeneration of Eqs. (71) and (89).

After all simplifications, the tensor of the defect conductivity takes the form

$$\mathbf{D} = E(\alpha_1^2\mathbf{1} - \alpha_2^2\mathbf{m}). \tag{17}$$

Obviously, the first length parameter α_1 is related with isotropic diffusion presented by the second-order identity tensor $\mathbf{1}$; the second length parameter α_2 is related with anisotropic diffusion presented by the normalized stress deviator $\mathbf{m}$. Thus, we correct the general isotropic diffusion term with the anisotropy induced by stresses.

It is worth mentioning that a slightly different discussion of the physical basis for equations of type (12) and (17) can be found in numerous works of Aifantis and his co-workers. Our mathematical development of the earlier Aifantis theory is in relaxing the form of the diffusion coefficient which was assumed to be a scalar in the original theory. Here, we propose the second-order defect conductivity tensor, which is generally stress-dependent, instead of the constant scalar diffusion coefficient.

Though a rough physical reasoning is unavoidable in developing a phenomenological theory it is always speculative. Those readers who are not fully satisfied with the arguments presented above may wish to alternatively consider the mechanism-based strain gra-

dient plasticity developed by Gao and Huang and their collaborators. They link the mesoscale kinematics to the dislocation structure directly. Though this achievement decreases the physical uncertainty of the phenomenological plasticity model the necessity to introduce a collection of physically unclear higher-order stresses, which are work-conjugate to the strain gradients, seems to increase the uncertainty back.

Considering the yield equation in the form (12) it must be remembered that the introduction of the spatial derivatives of the effective plastic strain requires additional boundary conditions on the surface of the plastic zone

$$\varepsilon_{\mathrm{p}} = 0 \quad \text{or} \quad \mathbf{g}\cdot\mathbf{n} = 0, \quad \text{on } \partial\Omega_{\mathrm{p}}. \tag{18}$$

The first condition corresponds to the constrained and the second to the non-constrained motion of defects on the proper boundary of a plastic zone. It is fortunate that the first condition is automatically satisfied on the boundaries of plastic zones inside the body. Thus, conditions (18) should be set on the general body boundaries

$$\varepsilon_{\mathrm{p}} = 0 \quad \text{or} \quad \mathbf{g}\cdot\mathbf{n} = 0, \quad \text{on } \partial\Omega. \tag{19}$$

Our treatment of boundary conditions follows that of Fleck and Hutchinson (2001) and we consider the elastic–plastic interface free of dislocations. Alternatively, Gudmundson (2004) suggests that dislocations are accumulated at the interface between the elastic and plastic phases. It is not clear in the latter case what serves as an obstacle for further intervention of the dislocations into the elastic region. It should be admitted, nonetheless, that physical connotation of the additional boundary conditions is a subtle matter. It is possible, for example that conditions (19) represent two extreme cases while many problems should require somewhat intermediate situations. The dislocation dynamic simulation can hopefully, shed light on the correct formulation of the continuum boundary conditions (19). Han et al. (2006) found, for example, that dislocations behaved similarly at the free surface and the substrate interface of a thin film subjected to a uniform applied stress (Fig. 7 of Han et al., 2006). This result based on the dislocation dynamic simulation is somewhat surprising. Definitely, the clarification of the formulation of boundary conditions is on agenda.

Completing the BVP formulation we setup the elastic/plastic loading/unloading (Kuhn–Tucker) conditions as usual

$$f \leqslant 0, \quad \dot{\varepsilon}_{\mathrm{p}} f = 0 \quad \text{and} \quad \dot{\varepsilon}_{\mathrm{p}} \geqslant 0. \tag{20}$$

Assuming $\alpha_1 = 0$ and $\alpha_2 = 0$ we arrive at the classical von Mises J_2 plasticity. The same effect is also achieved when the second gradients of the effective plastic strain are small. Setting $\alpha_2 = 0$ we obtain the Aifantis theory (see Aifantis, 1984; Muhlhaus and Aifantis, 1991).

3. Examples

We analyze simple shear, wire torsion, void growth, and beam bending in this section. The examples are solved semi-analytically. Such solutions are achievable because the load increases monotonically and no elastic unloading occurs. In this case, we can consider the elastic–plastic hardening starting from the very beginning of the load application. The latter means that we have to include the elastic range in the hardening curve or, in other words, to use the Ramberg–Osgood experimental curve for the total strain

$$\frac{\varepsilon}{\varepsilon_0} = \frac{\sigma_y}{\sigma_0} + \left(\frac{\sigma_y}{\sigma_0}\right)^n \tag{21}$$

with $\sigma_0 = E\varepsilon_0$ for a stress corresponding to the onset of the plastic deformation; n for a material parameter; and $\varepsilon = \sqrt{2\boldsymbol{\varepsilon} : \boldsymbol{\varepsilon}/3}$ for the effective strain. It will be shown below that it is possible to integrate the flow rule exactly and, consequently, to consider finite increments instead of the infinitesimal ones. Material parameters are common to all examples: the Poisson ratio is $v = 0.3$; the hardening parameter is $n = 5$; and the shear modulus is $G = E/2(1+v) = E/2.6$.

We should mention, besides, that though the described examples are often examined in the literature within various theoretical frameworks the specific solution procedures presented below are unique because the flow theory is considered and the total equilibrium condition is obeyed. Typically, the analogous solutions in the literature are based on the so-called deformation theory where no distinction between elastic and plastic deformations is made and/or the equilibrium conditions are obeyed incrementally only.

3.1. Simple shear

An infinite $-\infty \leqslant x_1 \leqslant \infty$ elastic–plastic layer $-l \leqslant x_2 \leqslant l$ in the state of plane strain is considered. Each face is bonded to a rigid substrate. The substrates undergo relative shear displacements $u_1(l) = \bar{u}$ and $u_1(-l) = -\bar{u}$. We will use the Cartesian frame with base vectors $\mathbf{k}_1 = (1,0,0)^{\mathrm{T}}$; $\mathbf{k}_2 = (0,1,0)^{\mathrm{T}}$; $\mathbf{k}_3 = (0,0,1)^{\mathrm{T}}$ and assume the following expression for the displacement field

$$\mathbf{u} = u(x_2)\mathbf{k}_1. \tag{22}$$

In this case, the total strain tensor takes form

$$\boldsymbol{\varepsilon} = \frac{1}{2}\frac{\partial u}{\partial x_2}(\mathbf{k}_1 \otimes \mathbf{k}_2 + \mathbf{k}_2 \otimes \mathbf{k}_1). \tag{23}$$

It is assumed that the plastic strain can be presented similarly

$$\boldsymbol{\varepsilon}^{\mathrm{p}} = \frac{1}{2}\beta_{\mathrm{p}}(x_2)(\mathbf{k}_1 \otimes \mathbf{k}_2 + \mathbf{k}_2 \otimes \mathbf{k}_1), \tag{24}$$

where β_{p} is unknown.

Based on (23) and (24) we have for the stresses tensor (5), effective stress (10) and dimensionless deviatoric stress (8) accordingly

$$\boldsymbol{\sigma} = \mathbf{s} = G(\partial u/\partial x_2 - \beta_{\mathrm{p}})(\mathbf{k}_1 \otimes \mathbf{k}_2 + \mathbf{k}_2 \otimes \mathbf{k}_1), \tag{25}$$

$$\sigma = \sqrt{3\mathbf{s} : \mathbf{s}/2} = \sqrt{3}G(\partial u/\partial x_2 - \beta_{\mathrm{p}}), \tag{26}$$

$$\mathbf{m} = \sqrt{3}(\mathbf{k}_1 \otimes \mathbf{k}_2 + \mathbf{k}_2 \otimes \mathbf{k}_1)/2. \tag{27}$$

Now, the flow rule (6) reduces to

$$\dot{\beta}_{\mathrm{p}} = \sqrt{3}\dot{\varepsilon}_{\mathrm{p}}. \tag{28}$$

Integrating it under condition $\varepsilon_{\mathrm{p}}(t=0) = \beta_{\mathrm{p}}(t=0) = 0$ we have

$$\beta_{\mathrm{p}} = \sqrt{3}\varepsilon_{\mathrm{p}}. \tag{29}$$

The equilibrium equation reads

$$\mathrm{div}\boldsymbol{\sigma} = G(\partial^2 u/\partial x_2^2 - \partial\beta_\mathrm{p}/\partial x_2)\mathbf{k}_1 = \mathbf{0}. \tag{30}$$

This equation is supplemented by the following boundary conditions with account of symmetry

$$\begin{cases} \mathbf{u}(x_2 = 0) = \mathbf{0}, \\ \mathbf{u}(x_2 = l) = \bar{u}\mathbf{k}_1. \end{cases} \tag{31}$$

Now, the yield condition (12) takes the following form

$$f = \sigma - \sigma_y(\varepsilon_\mathrm{p}) + \alpha_1^2 E\frac{\partial^2\varepsilon_\mathrm{p}}{\partial x_2^2} = 0. \tag{32}$$

This equation is supplemented by the following boundary conditions

$$\begin{cases} \frac{\partial\varepsilon_\mathrm{p}}{\partial x_2}(x_2 = 0) = 0, \\ \varepsilon_\mathrm{p}(x_2 = l) = 0. \end{cases} \tag{33}$$

Here the first condition is dictated by the symmetry of the plastic flow with respect to the middle plane while the second condition is imposed on the stiff boundary which prevents from any defect intervention.

Introducing the following set of parameters

$$y \equiv \frac{\beta_\mathrm{p}}{\varepsilon_0}, \quad x \equiv \frac{x_2}{l}, \quad z \equiv \frac{u}{l\varepsilon_0}, \quad q \equiv \frac{\alpha_1}{l}, \quad \sigma^* \equiv \frac{\sigma_y}{\sigma_0} = \frac{\sigma_y}{E\varepsilon_0}, \tag{34}$$

we can restate the boundary value problem (BVP) in the non-dimensional form

$$\frac{\partial^2 z}{\partial x^2} - \frac{\partial y}{\partial x} = 0, \tag{35}$$

$$\frac{\sqrt{3}}{2.6}\left(\frac{\partial z}{\partial x} - y\right) - \sigma^* + \frac{q^2}{\sqrt{3}}\frac{\partial^2 y}{\partial x^2} = 0, \tag{36}$$

$$\frac{1}{\sqrt{3}}\frac{\partial z}{\partial x} = \sigma^* + (\sigma^*)^n, \tag{37}$$

$$\begin{cases} z(x = 0) = 0, \\ z(x = 1) = \bar{z}, \end{cases} \tag{38}$$

$$\begin{cases} \frac{\partial y}{\partial x}(x = 0) = 0, \\ y(x = 1) = 0. \end{cases} \tag{39}$$

Here we have equations of equilibrium (35) and yield (36) with boundary conditions (38) and (39) accordingly. The Ramberg–Osgood curve given by (37) is not resolved analytically with respect to σ^* and can be considered as a mathematical constraint imposed on the variables involved in the BVP.

Finally, the shear traction S can be written in the dimensionless form as follows

$$\frac{S}{\varepsilon_0 G} = \frac{\partial z}{\partial x} - y = \text{constant}. \tag{40}$$

Boundary value problem (35)–(40) is discretized by using finite differences. The solution is visualized in Figs. 1 and 2 for various magnitudes of the dimensionless length-scale param-

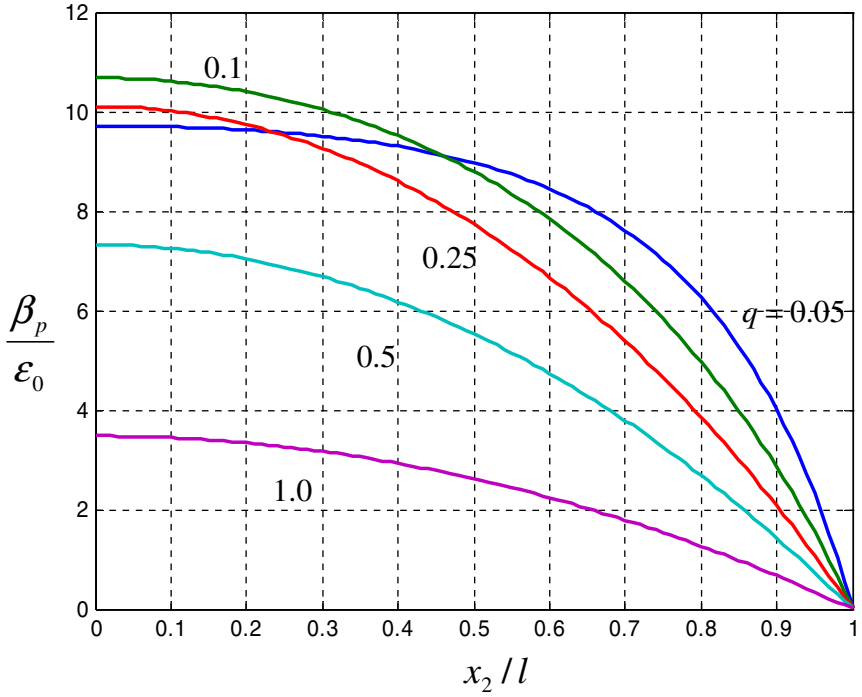

Fig. 1. Plastic shear distribution for half-layer for various values of the relative length parameter $q = \alpha_1/l$.

eter q. The stiffness of the shearing layer increases with the increase of the length parameter. The plastic shear decreases towards the fixed boundary as expected.

Our results presented in Figs. 1 and 2 are in a very good correspondence with the results of Fleck and Hutchinson (2001) presented in Figs. 1 and 2 of their paper. The qualitative similarity is striking. Some quantitative dissimilarity can be explained by slightly different theoretical formulations and solution methods.

3.2. Wire torsion

An elastic–plastic wire of radius a is considered. A cylindrical coordinate frame r, θ, z with unit base vectors $\mathbf{k}_r = (\cos\theta, \sin\theta, 0)^{\mathrm{T}}$; $\mathbf{k}_\theta = (-\sin\theta, \cos\theta, 0)^{\mathrm{T}}$; $\mathbf{k}_z = (0, 0, 1)^{\mathrm{T}}$ is used and the following expression for the displacement field is assumed

$$\mathbf{u} = r\alpha z \mathbf{k}_\theta, \tag{41}$$

where α is twist per unit length.

In this case, the total strain tensor takes form

$$\boldsymbol{\varepsilon} = \frac{1}{2} r\alpha (\mathbf{k}_\theta \otimes \mathbf{k}_z + \mathbf{k}_z \otimes \mathbf{k}_\theta). \tag{42}$$

We assume that the plastic strain can be presented similarly

$$\boldsymbol{\varepsilon}^{\mathrm{p}} = \frac{1}{2} \beta_{\mathrm{p}}(r) (\mathbf{k}_\theta \otimes \mathbf{k}_z + \mathbf{k}_z \otimes \mathbf{k}_\theta), \tag{43}$$

where β_{p} is unknown.

Based on (42) and (43) we have for the stresses tensor (5), effective stress (10) and dimensionless deviatoric stress (8) accordingly

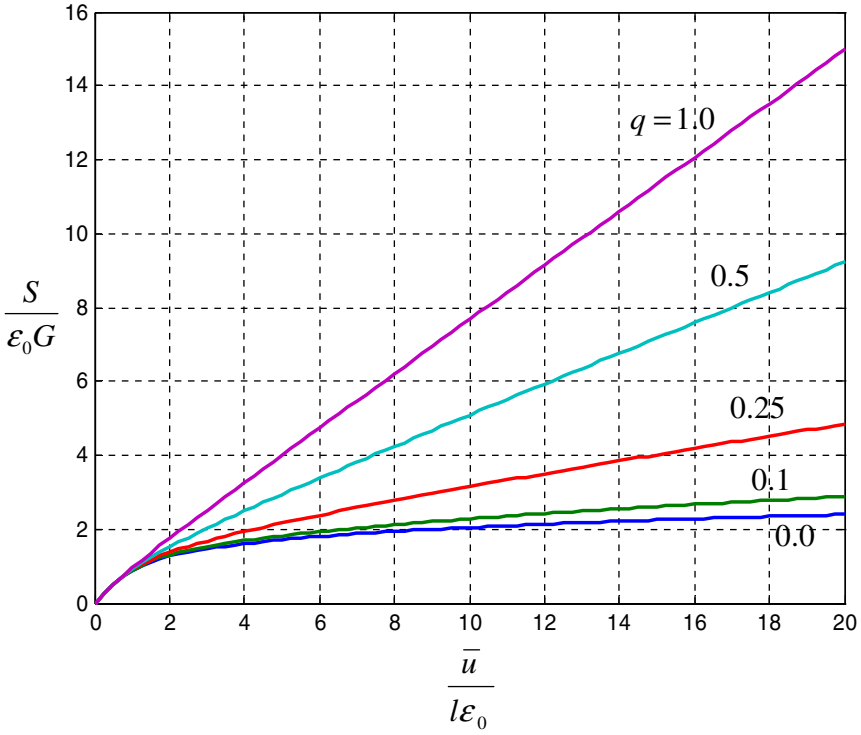

Fig. 2. Effect of the material length parameter on the relation between shear tractions and displacements for the elastic–plastic layer.

$$\boldsymbol{\sigma} = \mathbf{s} = G(\alpha r - \beta_{\mathrm{p}})(\mathbf{k}_\theta \otimes \mathbf{k}_z + \mathbf{k}_z \otimes \mathbf{k}_\theta), \tag{44}$$

$$\sigma = \sqrt{3\mathbf{s} : \mathbf{s}/2} = \sqrt{3}G(\beta - \beta_{\mathrm{p}}), \tag{45}$$

$$\mathbf{m} = \sqrt{3}(\mathbf{k}_\theta \otimes \mathbf{k}_z + \mathbf{k}_z \otimes \mathbf{k}_\theta)/2. \tag{46}$$

Now, the flow rule (6) reduces to

$$\dot{\beta}_{\mathrm{p}} = \sqrt{3}\dot{\varepsilon}_{\mathrm{p}}. \tag{47}$$

Integrating it under condition $\varepsilon_{\mathrm{p}}(t=0) = \beta_{\mathrm{p}}(t=0) = 0$ we have

$$\beta_{\mathrm{p}} = \sqrt{3}\varepsilon_{\mathrm{p}}. \tag{48}$$

The equilibrium condition is satisfied identically

$$\mathrm{div}\boldsymbol{\sigma} = \mathbf{0}, \tag{49}$$

as well as the boundary conditions of the traction-free wire surface

$$\boldsymbol{\sigma}\mathbf{k}_r = \mathbf{0}. \tag{50}$$

The boundary conditions at the edges of the wire should read

$$\begin{cases} \mathbf{u}(z=0) = \mathbf{0}, \\ \mathbf{u}(z=l) = r\alpha l \mathbf{k}_\theta = r\mathbf{A}\mathbf{k}_\theta, \end{cases} \tag{51}$$

where $A = \alpha l$ is prescribed.

Now, the yield condition (12) takes the following form

$$f = \sigma - \sigma_y(\varepsilon_{\mathrm{p}}) + \alpha_1^2 E\left(\frac{\partial^2 \varepsilon_{\mathrm{p}}}{\partial r^2} + \frac{\partial \varepsilon_{\mathrm{p}}}{r\partial r}\right) = 0. \tag{52}$$

This equation is supplemented by the following boundary conditions

$$\begin{cases} \frac{\partial \varepsilon_p}{\partial r}(r=0)=0, \\ \frac{\partial \varepsilon_p}{\partial r}(r=a)=0. \end{cases} \tag{53}$$

The first boundary condition in (53) is dictated by the symmetry of the problem and the necessity to suppress the singularity of the yield condition (52) at $r=0$. The second boundary condition manifests the zero defect flux at the free surface as opposed to the case of the fixed boundary where condition $(19)_1$ should be obeyed.

Introducing the following set of parameters

$$y \equiv \frac{\beta_p}{\varepsilon_0}, \quad x \equiv \frac{r}{a}, \quad z \equiv \frac{a\alpha}{\varepsilon_0}, \quad q \equiv \frac{\alpha_1}{a}, \quad \sigma^* \equiv \frac{\sigma_y}{\sigma_0} = \frac{\sigma_y}{E\varepsilon_0}, \tag{54}$$

we can restate the boundary value problem (BVP) in the non-dimensional form

$$\frac{\sqrt{3}}{2.6}(zx-y)-\sigma^*+\frac{q^2}{\sqrt{3}}\left(\frac{\partial^2 y}{\partial x^2}+\frac{\partial y}{x\partial x}\right)=0, \tag{55}$$

$$\frac{xz}{\sqrt{3}}=\sigma^*+(\sigma^*)^n, \tag{56}$$

$$\begin{cases} \frac{\partial y}{\partial x}(x=0)=0, \\ \frac{\partial y}{\partial x}(1)=0. \end{cases} \tag{57}$$

Here we have the equations of yield (55) with boundary conditions (57). The Ramberg–Osgood curve given by (56) is not resolved analytically with respect to σ^* and can be considered as a mathematical constraint imposed on the variables involved in the BVP.

Finally, the torque can be written as follows

$$T=\int_0^{2\pi}\int_0^a \sigma_{\theta z} r^2\,\mathrm{d}r\,\mathrm{d}\theta = 2\pi\int_0^a \sigma_{\theta z} r^2\,\mathrm{d}r = 2\pi G\int_0^a (r\alpha-\beta_p)r^2\,\mathrm{d}r, \tag{58}$$

or dimensionless

$$\frac{T}{\varepsilon_0 G a^3}=2\pi\int_0^1 (xz-\beta_p)x^2\,\mathrm{d}x \tag{59}$$

Boundary value problem (55)–(57) is discretized by using finite differences. The solution is given in Fig. 3 for various magnitudes of the dimensionless length-scale parameter q. As in the case of plastic shear considered in the previous section we have stiffening for the increasing value of the length parameter. It is interesting that both wire torsion and layer shearing are not affected by the second characteristic length. This happens because the defect flow is 'orthogonal' to the stress field in view of the constitutive equation for the defect flux (13) and (17). This is a feature of the considered constitutive model. A different model would not lead to this conclusion generally.

Our results presented in Fig. 3 are in a very good qualitative correspondence with (I) the results of Fleck and Hutchinson (2001) presented in Fig. 3 of their paper; (II) the results of Gudmundson (2004) presented in Fig. 1 of his paper; and (III) the results of Huang et al. (2000) presented in Fig. 3 of their paper. Some quantitative dissimilarity is expected because of the different theoretical formulations and solution methods.

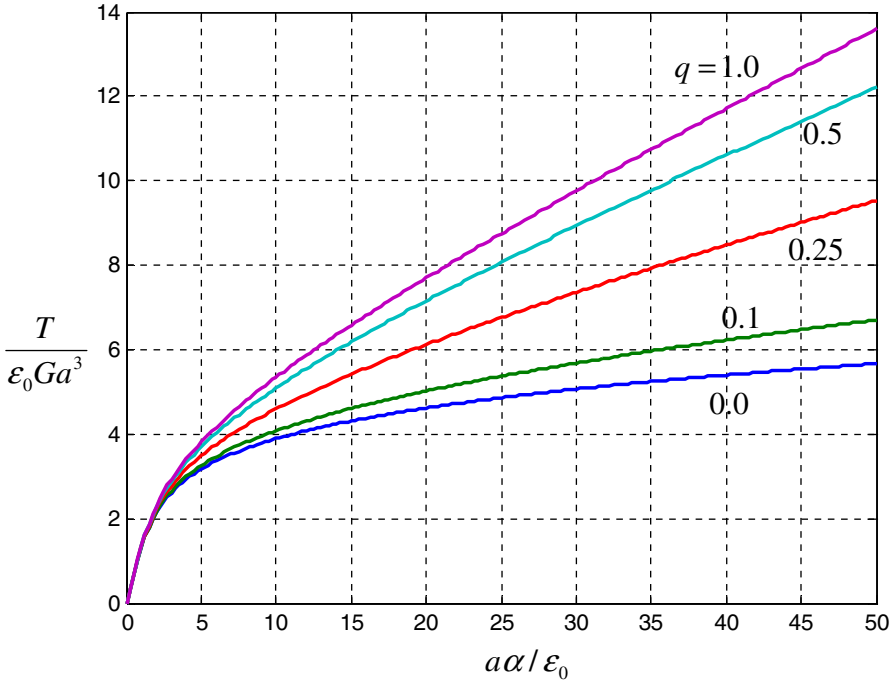

Fig. 3. Wire torsion: torque versus twist for varying characteristic length $q = \alpha_1/a$.

3.3. Void growth

Growth of an isolated spherical void of radius a inside an elastic–plastic incompressible continuum is considered. Spherical coordinate frame r, θ, ϕ with unit base vectors $\mathbf{k}_r = (\sin\theta\cos\phi, \sin\theta\sin\phi, \cos\theta)^{\mathrm{T}}$, $\mathbf{k}_\theta = (\cos\theta\cos\phi, \cos\theta\sin\phi, -\sin\theta)^{\mathrm{T}}$, $\mathbf{k}_\phi = (-\sin\phi, \cos\phi, 0)^{\mathrm{T}}$ is used.

The continuum incompressibility condition implies the following expression for the displacement field

$$\mathbf{u} = Ar^{-2}\mathbf{k}_r, \tag{60}$$

where A is an amplitude factor.

In this case, the total strain tensor takes form

$$\boldsymbol{\varepsilon} = Ar^{-3}(-2\mathbf{k}_r \otimes \mathbf{k}_r + \mathbf{k}_\theta \otimes \mathbf{k}_\theta + \mathbf{k}_\phi \otimes \mathbf{k}_\phi). \tag{61}$$

We assume that the plastic strain can be presented similarly

$$\boldsymbol{\varepsilon}^{\mathrm{p}} = \beta_{\mathrm{p}}(r)(-2\mathbf{k}_r \otimes \mathbf{k}_r + \mathbf{k}_\theta \otimes \mathbf{k}_\theta + \mathbf{k}_\phi \otimes \mathbf{k}_\phi), \tag{62}$$

where β_{p} is unknown.

Based on (61) and (62) we have for the stresses tensor (5), effective stress (10) and dimensionless deviatoric stress (8) accordingly

$$\boldsymbol{\sigma} = 2G(\beta - \beta_{\mathrm{p}})(-2\mathbf{k}_r \otimes \mathbf{k}_r + \mathbf{k}_\theta \otimes \mathbf{k}_\theta + \mathbf{k}_\phi \otimes \mathbf{k}_\phi), \tag{63}$$

$$\sigma = \sqrt{3\mathbf{s} : \mathbf{s}/2} = 6G(\beta - \beta_{\mathrm{p}}), \tag{64}$$

$$\mathbf{m} = (-2\mathbf{k}_r \otimes \mathbf{k}_r + \mathbf{k}_\theta \otimes \mathbf{k}_\theta + \mathbf{k}_\phi \otimes \mathbf{k}_\phi)/2. \tag{65}$$

Now, the flow rule (6) reduces to

$$\dot{\beta}_{\mathrm{p}} = \dot{\varepsilon}_{\mathrm{p}}/2. \tag{66}$$

Integrating it under condition $\varepsilon_{\mathrm{p}}(t=0) = \beta_{\mathrm{p}}(t=0) = 0$ we have

$$\beta_{\mathrm{p}} = \varepsilon_{\mathrm{p}}/2. \tag{67}$$

The equilibrium equation $\mathrm{div}(\boldsymbol{\sigma} - p\mathbf{1}) = \mathbf{0}$ reads

$$\frac{\partial(\sigma_{rr}-p)}{\partial r} + 2\frac{\sigma_{rr}-\sigma_{\theta\theta}}{r} = \frac{\partial(\sigma_{rr}-p)}{\partial r} + 3\frac{\sigma_{rr}}{r} = 0, \tag{68}$$

where p is the Lagrange multiplier enforcing the total incompressibility condition. Integrating the equilibrium equation we have

$$p(r) = \sigma_{rr}(r) + 3\int_a^r \frac{\sigma_{rr}}{r}\,\mathrm{d}r. \tag{69}$$

The following boundary conditions imposed on tractions should be obeyed

$$\begin{cases} \sigma_{rr}(a) - p(a) = 0, \\ \sigma_{rr}(b) - p(b) = -3\int_a^b \frac{\sigma_{rr}}{r}\,\mathrm{d}r = \sigma_\infty \quad (b \to \infty), \end{cases} \tag{70}$$

where the remote stress σ_∞ is prescribed.

Now, the yield condition (12) takes the following form

$$f = \sigma - \sigma_y(\varepsilon_{\mathrm{p}}) + E(\alpha_1^2 + \alpha_2^2)\frac{\partial^2\varepsilon_{\mathrm{p}}}{\partial r^2} + E(2\alpha_1^2 - \alpha_2^2)\frac{\partial\varepsilon_{\mathrm{p}}}{r\partial r} = 0. \tag{71}$$

This equation is supplemented by the following boundary conditions

$$\begin{cases} \frac{\partial\varepsilon_{\mathrm{p}}}{\partial r}(r=a) = 0, \\ \frac{\partial\varepsilon_{\mathrm{p}}}{\partial r}(r=b\to\infty) = 0. \end{cases} \tag{72}$$

We introduce the following set of parameters

$$y \equiv \frac{\beta_{\mathrm{p}}}{\varepsilon_0}, \quad x \equiv \frac{r}{a}, \quad z \equiv \frac{\Delta V}{V_0\varepsilon_0} = \frac{3A}{a^3\varepsilon_0}, \quad q_1 \equiv \frac{\alpha_1}{a}, \quad q_2 \equiv \frac{\alpha_2}{a}, \quad \sigma^* \equiv \frac{\sigma_y}{\sigma_0} = \frac{\sigma_y}{E\varepsilon_0}, \tag{73}$$

where the void volume changes have been designated as follows

$$V = (4/3)\pi(a + A/a^2)^3 \approx V_0 + \Delta V, \quad V_0 = 4\pi a^3/3, \quad \Delta V = 4\pi A. \tag{74}$$

Now, we can restate the boundary value problem (BVP) in the non-dimensional form

$$(zx^{-3} - 3y)/1.3 - \sigma^* + 2(q_1^2 + q_2^2)\frac{\partial^2 y}{\partial x^2} + 2(2q_1^2 - q_2^2)\frac{\partial y}{x\partial x} = 0, \tag{75}$$

$$2zx^3/3 = \sigma^* + (\sigma^*)^n, \tag{76}$$

$$\begin{cases} \frac{\partial y}{\partial x}(x=1) = 0, \\ \frac{\partial y}{\partial x}(x = b/a \to \infty) = 0. \end{cases} \tag{77}$$

Here we have the equation of yield (75) with boundary conditions (77) and the Ramberg–Osgood curve given by (76).

Finally, the remote stress can be written as follows

$$\frac{\sigma_\infty}{G\varepsilon_0} = 4\int_1^{b/a} (zx^{-3} - 3y)x^{-1}\,\mathrm{d}x. \tag{78}$$

Boundary value problem (75)–(77) is discretized by using finite differences. The solution is given in Figs. 4 and 5 for various magnitudes of the dimensionless length-scale parameters q_1 and q_2. The numerical solution was generated for various ratios b/a. It converges for

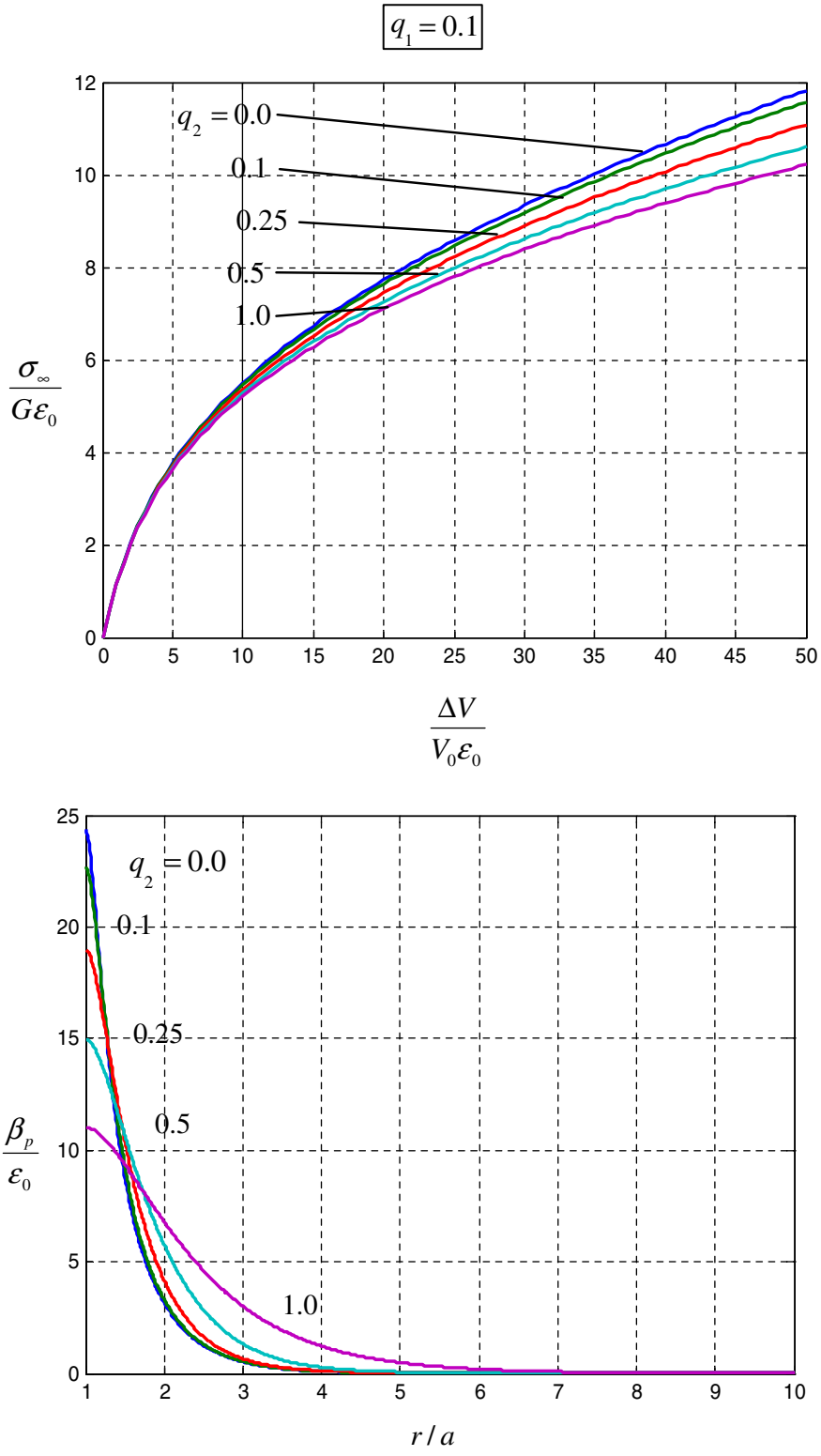

Fig. 4. Top: Remote stress as a function of the void volume expansion in the case of hydrostatic tension. Bottom: Plastic strain decay around the expanding void. All calculations have been done for the fixed first length parameter $q_1 = 0.1$ and the varying second length parameter $q_2 = 0; 0.1; 0.25; 0.5; 1$.

$b/a \geqslant 10$ already. Interestingly, the plastic strain decays quickly away from the void surface and the elastic–plastic boundary is readily observed. The increasing value of the first length parameter q_1 dominates the stiffening response of the growing void while the value

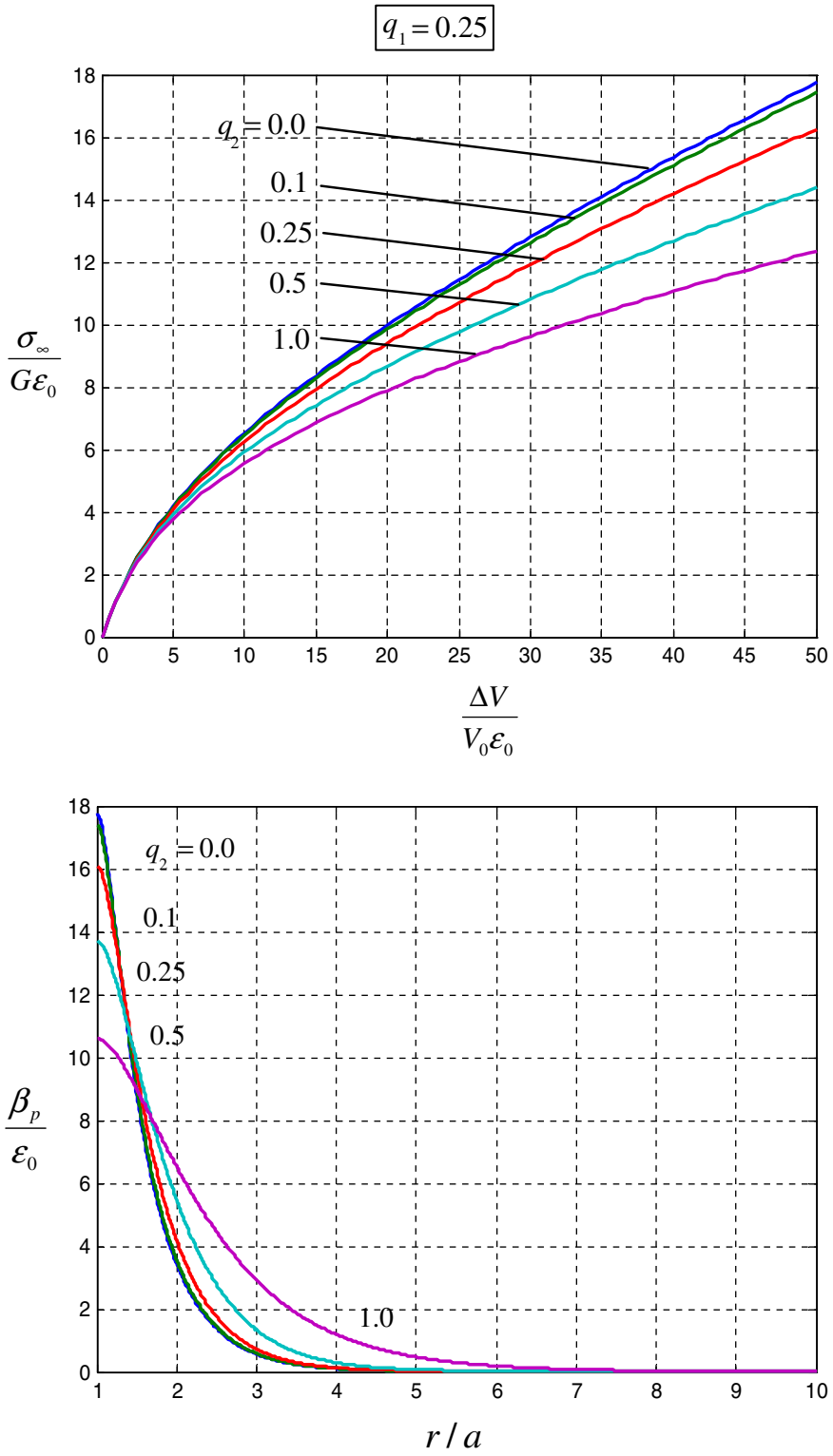

Fig. 5. Top: Remote stress as a function of the void volume expansion in the case of hydrostatic tension. Bottom: Plastic strain decay around the expanding void. All calculations have been done for the fixed first length parameter $q_1 = 0.25$ and the varying second length parameter $q_2 = 0; 0.1; 0.25; 0.5; 1$.

of the second length parameter q_2 can provide some diffusion of the plastic zone into the bulk. There is a stiffening–softening competition between these two parameters. Of course, such behavior is inherent in the proposed constitutive model of the defect flux. A different model would exhibit different features.

Our results presented in Figs. 4 and 5 are in a very good qualitative correspondence with (I) the results of Fleck and Hutchinson (2001) presented in Fig. 4 of their paper; (II) the results of Gudmundson (2004) presented in Figs. 3 and 4 of his paper; and (III) the results of Huang et al. (2000) presented in Figs. 5 and 7 of their paper. Some quantitative dissimilarity is expected because of the different theoretical formulations and solution methods.

3.4. Beam bending

Pure bending of an ultra-thin elastic–plastic beam of thickness h in the state of plane strain is considered. As in the previous section the material is assumed to be incompressible. The displacement field within the Cartesian frame is prescribed as follows

$$\mathbf{u} = \kappa x_1 x_2 \mathbf{k}_1 - \frac{1}{2}\kappa(x_1^2 + x_2^2)\mathbf{k}_2, \tag{79}$$

where κ is the curvature. In this case, the strain tensor takes form

$$\boldsymbol{\varepsilon} = \kappa x_2(\mathbf{k}_1 \otimes \mathbf{k}_1 - \mathbf{k}_2 \otimes \mathbf{k}_2). \tag{80}$$

We assume that the plastic strain can be presented similarly

$$\boldsymbol{\varepsilon}^{\mathrm{p}} = \beta_{\mathrm{p}}(x_2)(\mathbf{k}_1 \otimes \mathbf{k}_1 - \mathbf{k}_2 \otimes \mathbf{k}_2), \tag{81}$$

where β_{p} is unknown.

Based on (80) and (81) we have for the stresses tensor (5), effective stress (10) and dimensionless deviatoric stress (8) accordingly

$$\boldsymbol{\sigma} = \mathbf{s} = 2G(\kappa x_2 - \beta_{\mathrm{p}})(\mathbf{k}_1 \otimes \mathbf{k}_1 - \mathbf{k}_2 \otimes \mathbf{k}_2), \tag{82}$$

$$\sigma = \sqrt{3\mathbf{s} : \mathbf{s}/2} = 2\sqrt{3}G(\kappa x_2 - \beta_{\mathrm{p}}), \tag{83}$$

$$\mathbf{m} = \frac{\sqrt{3}}{2}(\mathbf{k}_1 \otimes \mathbf{k}_1 - \mathbf{k}_2 \otimes \mathbf{k}_2). \tag{84}$$

Now, the flow rule (6) reduces to

$$\dot{\beta}_{\mathrm{p}} = \frac{\sqrt{3}}{2}\dot{\varepsilon}_{\mathrm{p}}. \tag{85}$$

Integrating it under condition $\varepsilon_{\mathrm{p}}(t=0) = \beta_{\mathrm{p}}(t=0) = 0$ we have

$$\beta_{\mathrm{p}} = \frac{\sqrt{3}}{2}\varepsilon_{\mathrm{p}}. \tag{86}$$

The equilibrium equation reads

$$\mathrm{div}(\boldsymbol{\sigma} - p\mathbf{1}) = \frac{\partial(\sigma_{11} - p)}{\partial x_1}\mathbf{k}_1 + \frac{\partial(\sigma_{22} - p)}{\partial x_2}\mathbf{k}_2 = \mathbf{0}, \tag{87}$$

where p is the Lagrange multiplier enforcing the total incompressibility condition. Integrating the equilibrium equation and imposing zero traction boundary conditions on the top and the bottom of the beam we have

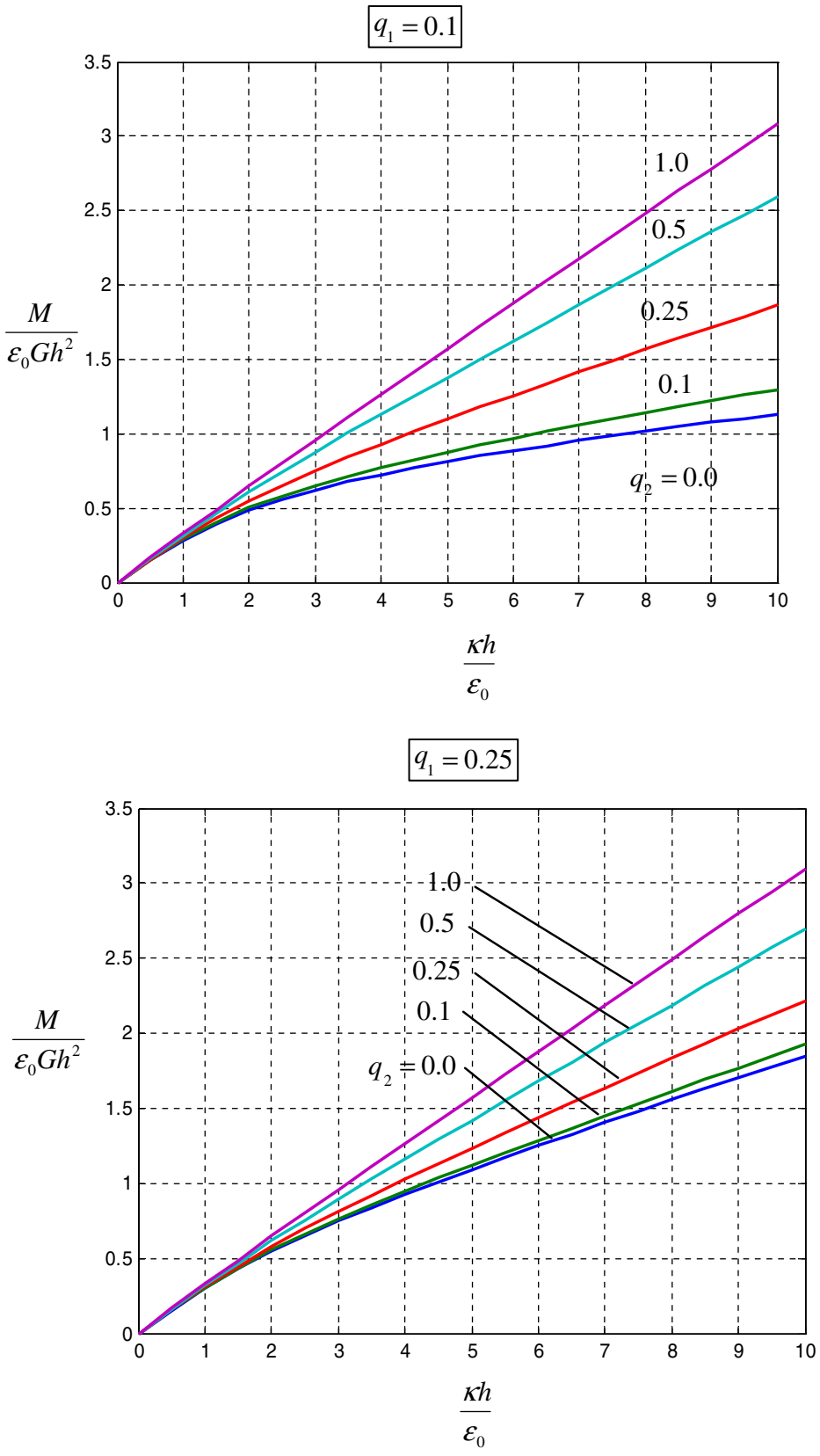

Fig. 6. Normalized bending moment versus normalized curvature of the bending beam for $q_1 = 0.1$; $q_2 = 0; 0.1; 0.25; 0.5; 1$ – top, and $q_1 = 0.25$; $q_2 = 0; 0.1; 0.25; 0.5; 1$ – bottom.

$$p(x_2) = \sigma_{22}(x_2). \tag{88}$$

Now, the yield condition (12) takes the following form

$$f = \sigma - \sigma_y(\varepsilon_p) + E\left(\alpha_1^2 + \frac{\sqrt{3}}{2}\alpha_2^2\right)\frac{\partial^2 \varepsilon_p}{\partial x_2^2} = 0. \tag{89}$$

This equation is supplemented by the following boundary conditions

$$\begin{cases} \varepsilon_p(x_2 = 0) = 0, \\ \frac{\partial \varepsilon_p}{\partial x_2}(x_2 = h/2) = 0. \end{cases} \tag{90}$$

Introducing the following set of parameters

$$y \equiv \frac{\beta_p}{\varepsilon_0}, \quad x \equiv \frac{x_2}{h}, \quad z \equiv \frac{\kappa h}{\varepsilon_0}, \quad q_1 \equiv \frac{\alpha_1}{h}, \quad q_2 \equiv \frac{\alpha_2}{h}, \quad \sigma^* \equiv \frac{\sigma_y}{\sigma_0} = \frac{\sigma_y}{E\varepsilon_0}, \tag{91}$$

we can restate the boundary value problem (BVP) in the non-dimensional form

$$\frac{f}{E\varepsilon_0} = \frac{2\sqrt{3}}{2.6}(zx - y) - \sigma^* + \left(q_1^2 + \frac{\sqrt{3}}{2}q_2^2\right)\frac{2}{\sqrt{3}}\frac{\partial^2 y}{\partial x^2} = 0, \tag{92}$$

$$2zx/\sqrt{3} = \sigma^* + (\sigma^*)^n, \tag{93}$$

$$\begin{cases} y(x = 0) = 0, \\ \frac{\partial y}{\partial x}(x = 1/2) = 0. \end{cases} \tag{94}$$

Here we have the equations of yield (92) with boundary conditions (94). The Ramberg–Osgood curve given by (93) is not resolved analytically with respect to σ^* and can be considered as a mathematical constraint imposed on the variables involved in the BVP.

Finally, the bending moment can be written as follows

$$M = \int_{-h/2}^{h/2} (\sigma_{11} - p)x_2 \, dx_2 = 4\int_{-h/2}^{h/2} G(\kappa x_2 - \beta_p)x_2 \, dx_2, \tag{95}$$

or dimensionless

$$\frac{M}{Gh^2\varepsilon_0} = 4\int_{-1/2}^{1/2} (zx - y)x \, dx. \tag{96}$$

The moment–curvature curve shown in Fig. 6 indicates that the increase of the second characteristic length leads to the stiffening response and it dominates the beam response for $q_2 \sim 1$.

Our results presented in Fig. 6 are in a very good qualitative correspondence with the results of Huang et al. (2000) presented in Fig. 1 of their paper. The quantitative dissimilarity is expected because of the different theoretical formulations and solution methods.

4. Comparison with the Fleck and Hutchinson (2001) theory

The 2001 Fleck–Hutchinson theory essentially inspired the present work in looking for a mathematically simple yet consistent theory of strain gradient plasticity that accommodates more than one characteristic length. In this sense, it is reasonable to make a more

detailed comparison of the present theory with the FH one. The basic idea of the FH theory which makes it different from and irreducible to all other SGP theories, including the one presented above, is the introduction of the generalized effective plastic strain

$$E_{\mathrm{p}} = \int \dot{E}_{\mathrm{p}}\,\mathrm{d}t, \tag{97}$$

$$\dot{E}_{\mathrm{p}}^2 = \dot{\varepsilon}_{\mathrm{p}}^2 + l_1^2\nabla\dot{\boldsymbol{\varepsilon}}_{\mathrm{p}}^{(1)}\vdots\nabla\dot{\boldsymbol{\varepsilon}}_{\mathrm{p}}^{(1)} + 4l_2^2\nabla\dot{\boldsymbol{\varepsilon}}_{\mathrm{p}}^{(2)}\vdots\nabla\dot{\boldsymbol{\varepsilon}}_{\mathrm{p}}^{(2)} + (8/3)l_3^2\nabla\dot{\boldsymbol{\varepsilon}}_{\mathrm{p}}^{(3)}\vdots\nabla\dot{\boldsymbol{\varepsilon}}_{\mathrm{p}}^{(3)}, \tag{98}$$

where the triple contraction of third-order tensors is defined symbolically: $\mathbf{A}\vdots\mathbf{A} \equiv A_{ijk}A_{ijk}$; and the gradient of the incremental plastic strain is decomposed in three mutually orthogonal tensors

$$\nabla\dot{\boldsymbol{\varepsilon}}^{\mathrm{p}} = \nabla\dot{\boldsymbol{\varepsilon}}_{\mathrm{p}}^{(1)} + \nabla\dot{\boldsymbol{\varepsilon}}_{\mathrm{p}}^{(2)} + \nabla\dot{\boldsymbol{\varepsilon}}_{\mathrm{p}}^{(3)}. \tag{99}$$

Taking the flow rule (6) into account it is possible to rewrite (98) as follows

$$\dot{E}_{\mathrm{p}}^2 = \dot{\varepsilon}_{\mathrm{p}}^2 + \nabla\dot{\varepsilon}_{\mathrm{p}}\cdot\mathbf{A}\nabla\dot{\varepsilon}_{\mathrm{p}} + \dot{\varepsilon}_{\mathrm{p}}\mathbf{B}\cdot\nabla\dot{\varepsilon}_{\mathrm{p}} + C\dot{\varepsilon}_{\mathrm{p}}^2, \tag{100}$$

where

$$\begin{cases} A_{ij} = l_1^2(\delta_{ij}/2 + 2m_{ip}m_{jp}/5) + e_{pir}m_{qr}(L_2^2e_{pjv}m_{qv} + L_3^2e_{qiv}m_{pv}), \\ B_i = l_1^2(4m_{pq}m_{pi,q}/3 - 8m_{ip}m_{pq,q}/15) + 2e_{pir}m_{qr}(L_2^2e_{puv}m_{qv,u} + L_3^2e_{quv}m_{pv,u}), \\ C = l_1^2(m_{ij,k}(m_{ij,k} + 2m_{jk,i}) - 4m_{ki,i}m_{kj,j}/15) + e_{pir}m_{qr,i}(L_2^2e_{puv}m_{qv,u} + L_3^2e_{quv}m_{pv,u}) \end{cases} \tag{101}$$

and e_{ijk} is a third-order permutation tensor; $L_2^2 = 4l_2^2/3 + 8l_3^2/5$; $L_3^2 = 4l_2^2/3 - 8l_3^2/5$.

Evidently, the generalized plastic strain includes gradient terms scaled by characteristic material lengths l_1, l_2, l_3. Although, generally, it is difficult to give a clear geometrical/physical interpretation to the plastic strain gradients and characteristic lengths some particular cases of deformation allow such an interpretation. FH theory suggests that the classical accumulated plastic strain ε_{p} should be replaced by the generalized plastic strain E_{p} in the yield/hardening condition. Using the notation of Section 2 of the present work we have according to FH

$$\sigma - \sigma_y(E_{\mathrm{p}}) - \mathrm{div}\mathbf{g}(E_{\mathrm{p}}) = 0. \tag{102}$$

The constitutive law for the yield stress $\sigma_y(E_{\mathrm{p}})$ is obtained from the experimental curve $\sigma_y(\varepsilon_{\mathrm{p}})$ by the direct substitution $\varepsilon_{\mathrm{p}} \to E_{\mathrm{p}}$. It is remarkable, however, that Fleck and Hutchinson do not provide a constitutive law for the defect flux (higher-order stress) vector $\mathbf{g}(E_{\mathrm{p}})$. Instead, they formulate an incremental variational principle which defines the *incremental* constitutive law

$$\dot{\mathbf{g}} = h(E_{\mathrm{p}})(\mathbf{A}\nabla\dot{\varepsilon}_{\mathrm{p}} + \dot{\varepsilon}_{\mathrm{p}}\mathbf{B}/2), \tag{103}$$

where $h = \partial\sigma_y/\partial E_{\mathrm{p}}$. Of course, the incremental formulation of the constitutive law differs from the straightforward formulation of Section 2 of the present work. This is especially important with regard to the presence of the normalized stress gradients $\nabla\mathbf{m}$ in $\mathbf{B}$ and C – (101). Incremental equations of yield/hardening of the FH theory include *the second spatial derivatives of stresses* (because of the divergence term) while the equilibrium equation includes only first derivatives of stresses. In this case, the order of the yield condition equation is higher than the order of the equilibrium equation. Assume, for example,

that boundary condition $\varepsilon_p = 0$ is given on $\partial\Omega$. In this case, the additional boundary conditions which should be imposed on the stress gradients seem to be lacking. This situation can be avoided, however, if one assumes $\mathbf{B} = \mathbf{0}$ and $C = 0$ in the FH setting. Indeed, it can be easily observed in (101) that tensor $\mathbf{A}$ depends only on the normalized stress deviator $\mathbf{m}$ and not on its gradients. The latter means that the yield equations will not increase the BVP order. Actually, tensor $\mathbf{A}$ can be considered as the defect conductivity tensor in the sense of the theory presented in Section 2: $\mathbf{D} = E\mathbf{A}$. Examination of such an assumption is of interest though it is beyond the scope of the present work. In summary, the present theory can be interpreted as a further simplification of the 2001 Fleck–Hutchinson theory.

5. Conclusions

A novel phenomenological theory of strain gradient plasticity is formulated to accommodate more than one material length parameter. This theory is an extension of the J_2 flow theory of metal plasticity to the length scale of microns. In a special case of one material length parameter the theory coincides with the Aifantis earlier theory. It is shown, however, how to introduce additional material length parameters without significantly complicating the SGP formulation. The necessity of introducing at least two material length parameters emerges from the recent experimental observations (see Fleck and Hutchinson, 2001). The theory developed in the present work is, to the best of our knowledge, the simplest one among the available theories involving more than one material length parameter. It is worth noting that the main problem of creating an attractive SGP theory is to find a right balance between the mathematical sophistication and physical clarity. Some SGP theories enjoy elegant and consistent mathematical structure of generalized continua. It is difficult, however, to interpret the new variables involved in such theories as, for example, higher-order (microscopic) stresses in simple physical terms. On the other hand, an attempt to oversimplify mathematics behind SGP can lead to inconsistency as in the case of lower-order strain gradient plasticity. It was attempted in the present work to move towards the balance between mathematics and physics. No higher-order stresses are involved in general. The only variable in our theory that corresponds to a higher-order stress in the theories of Fleck and Hutchinson (2001) or Gurtin (2000) is vector $\mathbf{g}$ in (12). It seems, however, that its physical interpretation as a vector of defect flux is more attractive than its interpretation as a higher-order/microscopic stress. Evidently, Eq. (19) provides the necessary additional boundary conditions providing mathematical consistency of the theory.

It is important to emphasize that the following basic physical assumption provides mathematical simplicity of the presented theory. It is assumed that the defect flux depends explicitly on the stress field in addition to being proportional to the gradient of the defect density (effective plastic strain). Such dependence is provided by the presence of a stress tensor (or/and its invariants) in the defect conductivity tensor. In other words, stresses make the defect diffusion anisotropic. The induced anisotropy does not necessarily affect the defect flow. As it appears in the considered examples of simple shear and wire torsion the gradient of the defect density can be orthogonal to the normalized deviatoric stress and no anisotropic defect diffusion takes place. On the contrary, in the cases of void growth and beam bending the stress-induced anisotropy can significantly affect the mechanical response.

Another distinct advantage of the considered theory over other existing SGP theories is simplicity of its numerical implementation – see Appendix. The weak formulation is based on two unknowns – the displacement vector field and a scalar field of the effective plastic strain. We modified the integration algorithm proposed by de Borst and Muhlhaus (1992) and de Borst and Pamin (1996) in order to adapt the proposed SGP framework. Considered numerical examples, where a comparison with analytical solutions is available, demonstrate computational efficiency of the algorithm.

Our results of the analysis of wire torsion, layer shearing, void growth, and beam bending are qualitatively similar to the results of other authors listed in the references though some features have to be discussed. The problems of wire torsion and simple shear include only one active length parameter as in most other theories and the wire torsion experiment can be used to calibrate the first length parameter, α_1. The problems of void growth and beam bending include both length parameters, α_1 and α_2. The void growth simulation reveals the stiffening–softening competition concerning the role of the first and the second material lengths correspondingly. The increase of the first material length parameter generally leads to the stiffening response of the growing void while the increase of the second material length parameter leads to softening of response of the void. In the latter case the elastic–plastic boundary moves deeper in the bulk and the maximum plastic strain at the void edge decreases or, in other words, the plastic boundary layer around the void gets wider while the plastic strain relaxes. In contrast to the void growth problem, the second length parameter serves as a stiffening factor similar to the first length parameter in the case of the beam bending. Moreover, the second length parameter can dominate the overall response of the beam. The latter makes it attractive to use the beam bending experiment for calibration. Stolken and Evans (1998) performed such experiments fitting the material length parameter of the earlier Fleck–Hutchinson theory. Unfortunately, the experiment implies large rotations of the beam fibers while the theory assumes the rotations to be small. It seems that any theory, including the present one, should be extended to large rotations before it can be used for the interpretation of the beam bending experiments. Another potential source of experimental data on the calibration of the second length parameter is the indentation analysis. Begley and Hutchinson (1998) used the deformation version of the earlier Fleck–Hutchinson theory for the FE analysis of microindentation. Their results reveal that the FE approach is possible but not trivial way to calibrate the second length parameter.

Appendix A

The examples in Section 3 were considered (semi-)analytically and, in this appendix, we develop a more general finite element procedure following de Borst and Muhlhaus (1992) and de Borst and Pamin (1996) with slight modifications for adapting the present formulation of SGP. It should be noted, however, that alternative finite element approaches have been presently developed by Han et al. (2007) in the context of the gradient formulation of large strain crystal plasticity.

Consider the weak form of the incremental equilibrium equation

$$\int_{\Omega} \delta\dot{\mathbf{u}} \cdot \mathrm{div}\dot{\boldsymbol{\sigma}}\, \mathrm{d}V = 0, \tag{A.1}$$

where δ designates a virtual quantity and the dot designates an increment of a quantity. Applying the divergence theorem to (A.1) we have

$$\int_{\Omega} \delta\dot{\boldsymbol{\varepsilon}} : \dot{\boldsymbol{\sigma}} \, \mathrm{d}V - \int_{\partial\Omega} \delta\dot{\mathbf{u}} \cdot \dot{\bar{\mathbf{t}}} \, \mathrm{d}A = 0, \tag{A.2}$$

where

$$\dot{\boldsymbol{\varepsilon}} = (\nabla\dot{\mathbf{u}} + \nabla\dot{\mathbf{u}}^{\mathrm{T}})/2. \tag{A.3}$$

Now we consider the weak incremental form of the yield condition (12)

$$\int_{\Omega} \delta\dot{\varepsilon}_{\mathrm{p}}(\dot{\sigma} - \dot{\sigma}_y - \mathrm{div}\dot{\mathbf{g}}) \mathrm{d}V = 0. \tag{A.4}$$

Applying the divergence theorem to (A.4) and accounting for the boundary conditions (19) we have

$$\int_{\Omega} (\delta\dot{\varepsilon}_{\mathrm{p}}\dot{\sigma} - \delta\dot{\varepsilon}_{\mathrm{p}}\dot{\sigma}_y + \nabla\delta\dot{\varepsilon}_{\mathrm{p}} \cdot \dot{\mathbf{g}}) \mathrm{d}V = 0, \tag{A.5}$$

where

$$\dot{\sigma} = \frac{\partial\sigma}{\partial\boldsymbol{\sigma}} : \dot{\boldsymbol{\sigma}} = \mathbf{m} : \dot{\boldsymbol{\sigma}}, \tag{A.6}$$

$$\dot{\sigma}_y = \frac{\partial\sigma_y}{\partial\varepsilon_{\mathrm{p}}}\dot{\varepsilon}_{\mathrm{p}} \equiv h(\varepsilon_{\mathrm{p}})\dot{\varepsilon}_{\mathrm{p}}, \tag{A.7}$$

$$\dot{\mathbf{g}} = \frac{\partial\mathbf{g}}{\partial\boldsymbol{\sigma}} : \dot{\boldsymbol{\sigma}} + \frac{\partial\mathbf{g}}{\partial\nabla\varepsilon_{\mathrm{p}}}\nabla\dot{\varepsilon}_{\mathrm{p}}. \tag{A.8}$$

Substituting (A.6)–(A.8) in (A.5) we have

$$\int_{\Omega} (\delta\dot{\varepsilon}_{\mathrm{p}}\mathbf{m} : \dot{\boldsymbol{\sigma}} - \delta\dot{\varepsilon}_{\mathrm{p}}h(\varepsilon_{\mathrm{p}})\dot{\varepsilon}_{\mathrm{p}} + \nabla\delta\dot{\varepsilon}_{\mathrm{p}} \cdot [(\partial\mathbf{g}/\partial\boldsymbol{\sigma}) : \dot{\boldsymbol{\sigma}} + (\partial\mathbf{g}/\partial\nabla\varepsilon_{\mathrm{p}})\nabla\dot{\varepsilon}_{\mathrm{p}}]) \mathrm{d}V = 0, \tag{A.9}$$

Finally, we substitute the incremental Hooke law (5) with account of flow rule (6)

$$\dot{\boldsymbol{\sigma}} = \mathbf{C} : (\dot{\boldsymbol{\varepsilon}} - \dot{\varepsilon}_{\mathrm{p}}\mathbf{m}) \tag{A.10}$$

in the weak form of the incremental equations of equilibrium (A.2) and yield (A.9) accordingly

$$\int_{\Omega} \delta\dot{\boldsymbol{\varepsilon}} : \mathbf{C} : (\dot{\boldsymbol{\varepsilon}} - \dot{\varepsilon}_{\mathrm{p}}\mathbf{m}) \mathrm{d}V - \int_{\partial\Omega} \delta\dot{\mathbf{u}} \cdot \dot{\bar{\mathbf{t}}} \mathrm{d}A = 0, \tag{A.11}$$

$$\int_{\Omega} (\delta\dot{\varepsilon}_{\mathrm{p}}\mathbf{m} : \mathbf{C} : (\dot{\boldsymbol{\varepsilon}} - \dot{\varepsilon}_{\mathrm{p}}\mathbf{m}) - \delta\dot{\varepsilon}_{\mathrm{p}}h(\varepsilon_{\mathrm{p}})\dot{\varepsilon}_{\mathrm{p}} + \nabla\delta\dot{\varepsilon}_{\mathrm{p}} \cdot [\mathbf{R} : \mathbf{C} : (\dot{\boldsymbol{\varepsilon}} - \dot{\varepsilon}_{\mathrm{p}}\mathbf{m}) + \mathbf{r}\nabla\dot{\varepsilon}_{\mathrm{p}}]) \mathrm{d}V = 0. \tag{A.12}$$

The explicit expressions are obtained for the derivatives of the dislocation flux in view of assumptions (13) and (17)

$$\mathbf{R} \equiv \frac{\partial\mathbf{g}}{\partial\boldsymbol{\sigma}} = \frac{3E\alpha_2^2}{2\sigma}\left(\mathbf{1} \otimes \nabla\varepsilon_{\mathrm{p}} - \frac{1}{3}\nabla\varepsilon_{\mathrm{p}} \otimes \mathbf{1} - \frac{2}{3}(\mathbf{m}\nabla\varepsilon_{\mathrm{p}}) \otimes \mathbf{m}\right), \tag{A.13}$$

$$\mathbf{r} \equiv \frac{\partial\mathbf{g}}{\partial\nabla\varepsilon_{\mathrm{p}}} = -E(\alpha_1^2\mathbf{1} - \alpha_2^2\mathbf{m}). \tag{A.14}$$

The weak formulation (A.11)–(A.14) includes only unknown increments of displacements and effective plastic strain, which can be approximated spatially by using the following spatial discretization

$$u_i(\mathbf{x}) = \sum_I N_i^I(\mathbf{x}) a^I; \quad \dot{u}_i(\mathbf{x}) = \sum_I N_i^I(\mathbf{x}) \dot{a}^I; \quad \delta\dot{u}_i(\mathbf{x}) = \sum_I N_i^I(\mathbf{x}) \delta\dot{a}^I, \tag{A.15}$$

$$\varepsilon_{\mathrm{p}}(\mathbf{x}) = \sum_I H^I(\mathbf{x}) b^I; \quad \dot{\varepsilon}_{\mathrm{p}}(\mathbf{x}) = \sum_I H^I(\mathbf{x}) \dot{b}^I; \quad \delta\dot{\varepsilon}_{\mathrm{p}}(\mathbf{x}) = \sum_I H^I(\mathbf{x}) \delta\dot{b}^I, \tag{A.16}$$

where $N_i^I(\mathbf{x})$ and $H^I(\mathbf{x})$ are the shape functions for the displacement and effective plastic strain fields accordingly.

Substituting (A.15) and (A.16) in (A.11)–(A.14) and zeroing the coefficients of independent variations we arrive at the following matrix equation

$$\begin{bmatrix} \mathbf{K}_{aa} & \mathbf{K}_{ab} \\ \mathbf{K}_{ba} & \mathbf{K}_{bb} \end{bmatrix} \begin{Bmatrix} \dot{\mathbf{a}} \\ \dot{\mathbf{b}} \end{Bmatrix} = \begin{Bmatrix} \dot{\mathbf{q}}_a \\ \dot{\mathbf{q}}_b \end{Bmatrix}. \tag{A.17}$$

Here the matrix entries take the form

$$K_{aa}^{IJ} = \int_V N_{i,j}^I C_{ijkl} N_{k,l}^J \, \mathrm{d}V, \tag{A.18}$$

$$K_{ab}^{IJ} = -\int_V N_{i,j}^I C_{ijkl} m_{kl} H^J \, \mathrm{d}V, \tag{A.19}$$

$$K_{ba}^{IJ} = \int_V (H^I m_{ij} + H_{,s}^I R_{sij}) C_{ijkl} N_{k,l}^J \, \mathrm{d}V, \tag{A.20}$$

$$K_{bb}^{IJ} = \int_V (H_{,i}^I r_{ij} H_{,j}^J - (H^I m_{ij} + H_{,s}^I R_{sij}) C_{ijkl} m_{kl} H^J - H^I h H^J) \, \mathrm{d}V, \tag{A.21}$$

where

$$R_{sij} = \frac{3E\alpha_2^2}{2\sigma} \left(\delta_{si} \sum_L H_{,j}^L b^L - \frac{1}{3} \delta_{ij} \sum_L H_{,s}^L b^L - \frac{2}{3} m_{ij} m_{sn} \sum_L H_{,n}^L b^L \right), \tag{A.22}$$

$$r_{ij} = -E(\alpha_1^2 \delta_{ij} - \alpha_2^2 m_{ij}). \tag{A.23}$$

Comma is used to designate a partial derivative: $(\dots)_{,i} \equiv \partial(\dots)/\partial x_i$ and summation from 1 to 3 over the repeated subscripts is implied.

The entries on the right-hand side of (A.17) take the form

$$\dot{q}_a^I = \int_\Omega N_i^I \dot{\bar{t}}_i \, \mathrm{d}\Omega, \tag{A.24}$$

$$\dot{q}_b^I = 0. \tag{A.25}$$

This loading vector, however, gives the solution of a purely incremental problem. The latter is of limited interest since a significant departure from equilibrium can occur. In order to solve the complete BVP we have to consider the left-hand side of (A.17) as the tangent approximation of the equilibrium path of the elastic–plastic body in its state space. The right-hand side of (A.17) should provide an iterative residual

$$\dot{q}_a^I = \int_{\partial\Omega} N_i^I (\bar{t}_i + \dot{\bar{t}}_i) \mathrm{d}A - 1/2 \int_\Omega (N_{i,j}^I + N_{j,i}^I) \bar{\sigma}_{ij} \, \mathrm{d}V, \tag{A.26}$$

$$\dot{q}_b^I = -\int_V H^I \bar{f} \, \mathrm{d}V, \tag{A.27}$$

where $\bar{t}_i$, $\bar{\sigma}_{ij}$, $\bar{f}$ are the values accumulated in previous increments.

After solving (A.17) it is necessary to update variables $\mathbf{a} \leftarrow \mathbf{a} + \dot{\mathbf{a}}; \mathbf{b} \leftarrow \mathbf{b} + \dot{\mathbf{b}}$, the tangent stiffness matrix, and the right-hand side of (A.17) properly. This proceeds until a global convergence criterion is met. Thus applying the load *incrementally* we return to the equilibrium path *iteratively*. The computational algorithm is summarized below where the first upper index in parentheses designates the increment number while the second index designates the iteration number:

- Input (after the $(n-1)$th increment):

$$\mathbf{K}_{aa}^{(n-1)}, \mathbf{K}_{ab}^{(n-1)}, \mathbf{K}_{ba}^{(n-1)}, \mathbf{K}_{bb}^{(n-1)}, \mathbf{a}^{(n-1)}, \mathbf{b}^{(n-1)}, \mathbf{q}_a^{(n-1)}, \mathbf{q}_b^{(n-1)}.$$

- Onset of the nth increment:

$$\mathbf{K}_{aa}^{(n,0)} = \mathbf{K}_{aa}^{(n-1)}, \quad \mathbf{K}_{ab}^{(n,0)} = \mathbf{K}_{ab}^{(n-1)}, \quad \mathbf{K}_{ba}^{(n,0)} = \mathbf{K}_{ba}^{(n-1)}, \quad \mathbf{K}_{bb}^{(n,0)} = \mathbf{K}_{bb}^{(n-1)},$$
$$\mathbf{a}^{(n,0)} = \mathbf{a}^{(n-1)}, \quad \mathbf{b}^{(n,0)} = \mathbf{b}^{(n-1)}, \quad \dot{\mathbf{a}}^{(n,0)} = \mathbf{0}, \quad \dot{\mathbf{b}}^{(n,0)} = \mathbf{0}$$
$$\mathbf{q}_a^{(n,0)} = \mathbf{q}_a^{(n-1)} + \text{load increment}, \quad \mathbf{q}_b^{(n,0)} = \mathbf{q}_b^{(n-1)}.$$

- Iterative loop $i = 1, 2, \ldots$ to meet the global convergence criterion:
  - Solve:

$$\begin{bmatrix} \mathbf{K}_{aa}^{(n,i-1)} & \mathbf{K}_{ab}^{(n,i-1)} \\ \mathbf{K}_{ba}^{(n,i-1)} & \mathbf{K}_{bb}^{(n,i-1)} \end{bmatrix} \begin{Bmatrix} \tilde{\mathbf{a}} \\ \tilde{\mathbf{b}} \end{Bmatrix} = \begin{Bmatrix} \mathbf{q}_a^{(n,i-1)} \\ \mathbf{q}_b^{(n,i-1)} \end{Bmatrix}.$$

  - Update:

$$\dot{\mathbf{a}}^{(n,i)} = \dot{\mathbf{a}}^{(n,i-1)} + \tilde{\mathbf{a}}, \quad \mathbf{a}^{(n,i)} = \mathbf{a}^{(n,0)} + \dot{\mathbf{a}}^{(n,i)},$$
$$\dot{\mathbf{b}}^{(n,i)} = \dot{\mathbf{b}}^{(n,i-1)} + \tilde{\mathbf{b}}, \quad \mathbf{b}^{(n,i)} = \mathbf{b}^{(n,0)} + \dot{\mathbf{b}}^{(n,i)},$$
$$\dot{\varepsilon}_{kl}^{(n,i)} = 0.5(\mathbf{N}_{k,l}^{\mathrm{T}} + \mathbf{N}_{l,k}^{\mathrm{T}})\dot{\mathbf{a}}^{(n,i)}, \quad \mathbf{N}_{k,l}^{\mathrm{T}} = \{N_{k,l}^1, N_{k,l}^2, \ldots\},$$
$$\dot{\varepsilon}_{\mathrm{p}}^{(n,i)} = \mathbf{H}^{\mathrm{T}}\dot{\mathbf{b}}^{(n,i)}, \quad \mathbf{H}^{\mathrm{T}} = \{H^1, H^2, \ldots\},$$
$$\sigma_{kl}^{\mathrm{trial}} = \sigma_{kl}^{(n,0)} + C_{klst}\dot{\varepsilon}_{st}^{(n,i)},$$
$$\text{If} f(\sigma_{kl}^{\mathrm{trial}}, \mathbf{b}^{(n,i)}) \geqslant 0,$$
$$\text{then plasticity}: \quad \sigma_{kl}^{(n,i)} = \sigma_{kl}^{\mathrm{trial}} - \dot{\varepsilon}_{\mathrm{p}}^{(n,i)} C_{klst} m_{st}^{\mathrm{trial}},$$
$$\text{else elasticity}: \quad \sigma_{kl}^{(n,i)} = \sigma_{kl}^{\mathrm{trial}}.$$

To validate the integration algorithms we considered all numerical examples of the previous section within the finite element framework developed above. The wire torsion problem was considered in 1D and 2D formulations. We examined the coarse (150 elements) and fine (600 elements) meshes of linear triangles in the 2D formulation – Fig. A1 – and the 100 linear elements in the 1D formulation. The load was applied in 50 increments and the convergence to equilibrium did not require more than seven iterations within the increment. The results of numerical simulations are presented in

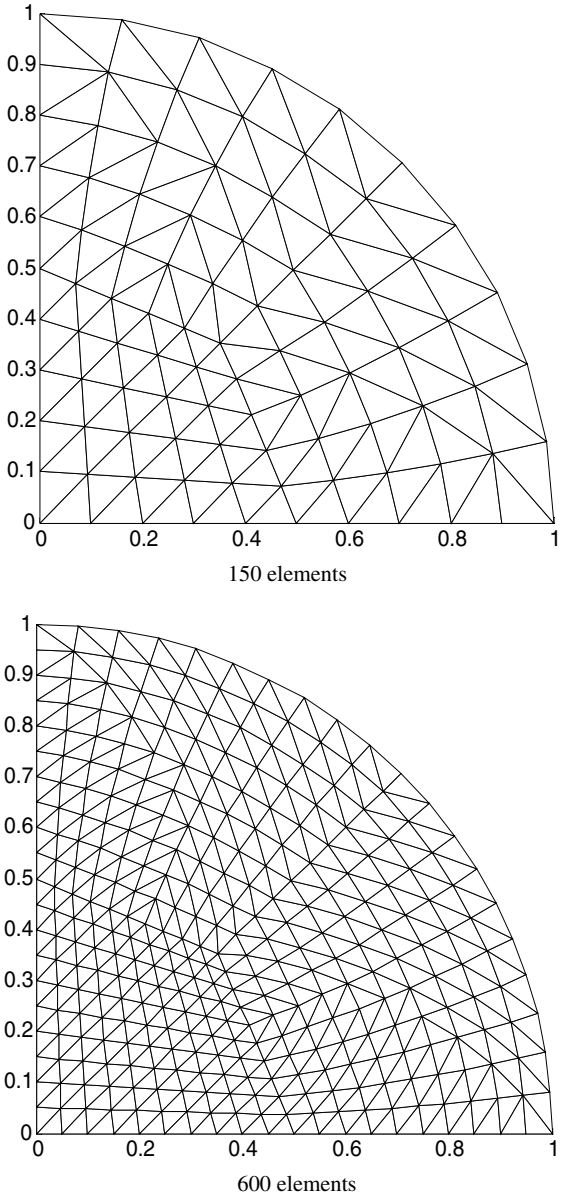

Fig. A1. 2D meshes of linear finite elements for the solution of the wire torsion problem.

Fig. A2 including the analytical solution of the previous section. It is readily seen that various curves practically coincide. In simulations of other problems – Figs. A3–A5 – we accounted for the assumed symmetries and considered 1D meshes with the linear shape functions. One hundred elements were used in all cases with the varying number of load increments: 50 for the void growth; 40 for the simple shear; 20 for the beam bending. The number of iterations within the load increment did not exceed seven in all cases. As in the case of the wire torsion a very close resemblance between the FE and analytical solutions has been observed. In summary the developed FE scheme provides satisfactory results for simulation of the examples considered in the previous section. It should be noted that the slight difference between the analytical and FE solutions in Figs. A4 and A5 can be explained by the fact that the analytical solution was based on the total stress–strain curve (21) while the numerical solution operates the plastic hardening only: $h = \partial\sigma_y/\partial\varepsilon_{\mathrm{p}} = (E/n)(\varepsilon_{\mathrm{p}}/\varepsilon_0)^{1/n-1}$.

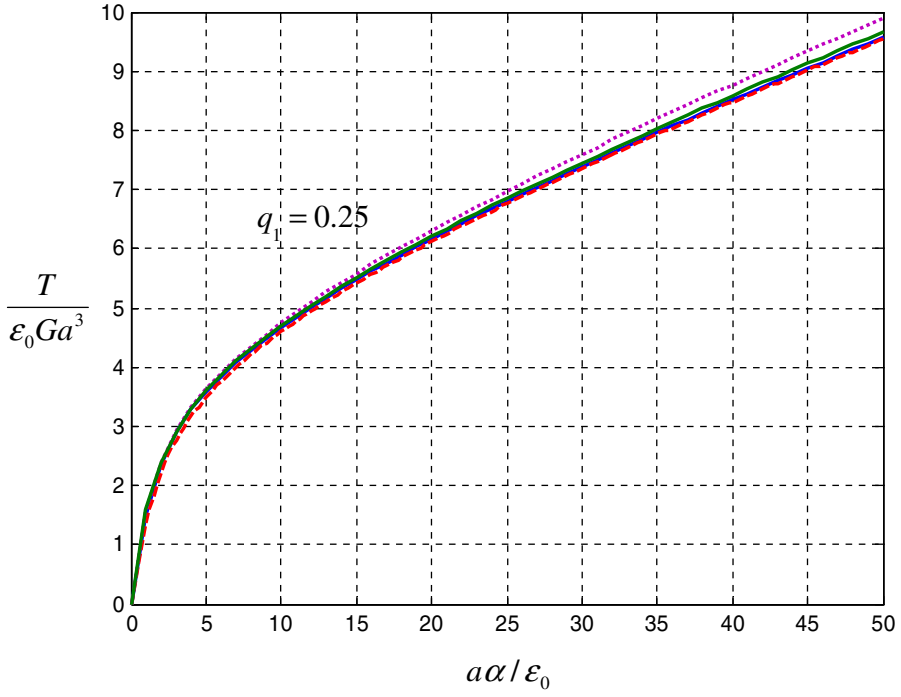

Fig. A2. Wire torsion. Comparison of analytical and FE solutions: analytical solution – dashed red line in webversion; 100 1D elements – solid blue line in webversion; 150 2D elements – dotted purple line in webversion; 600 2D elements – solid green line in webversion.

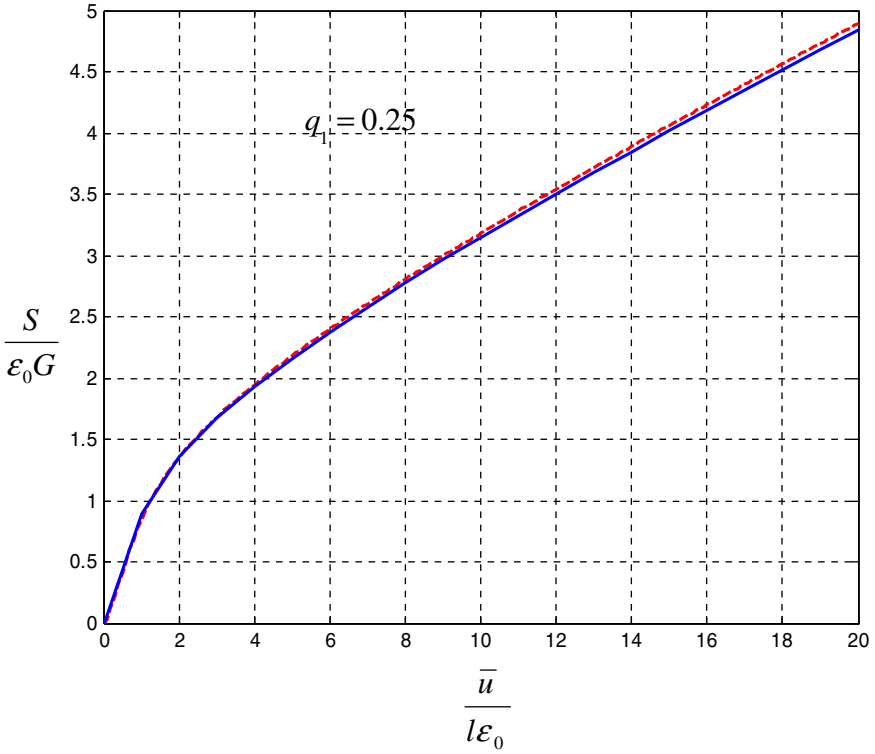

Fig. A3. Simple shear: analytical solution – dashed red line in webversion; 100 1D elements – solid blue line in webversion.

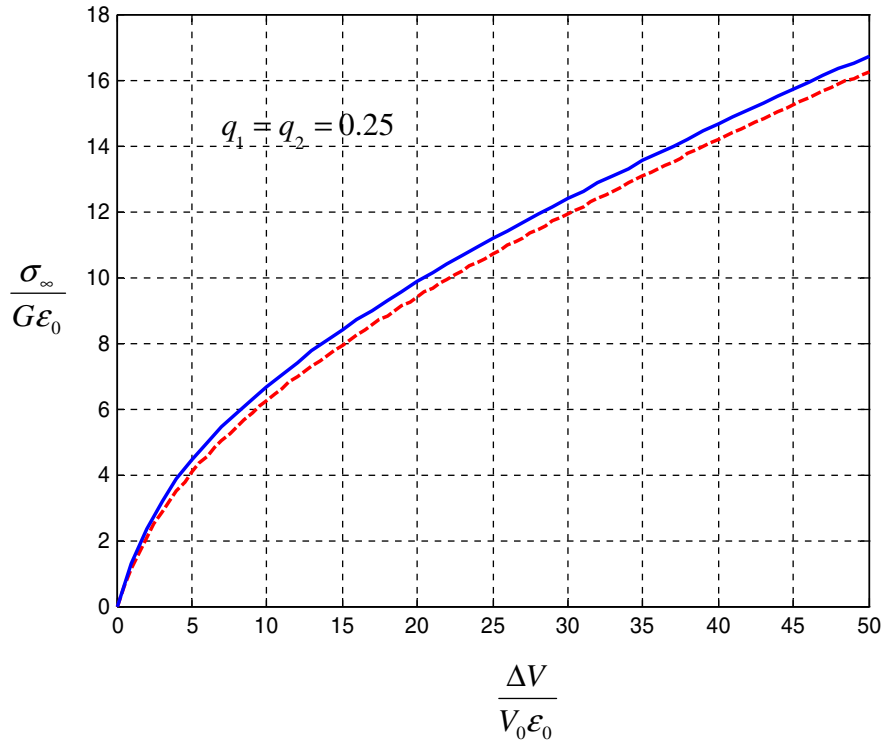

Fig. A4. Void growth: analytical solution – dashed red line in webversion; 100 1D elements – solid blue line in webversion.

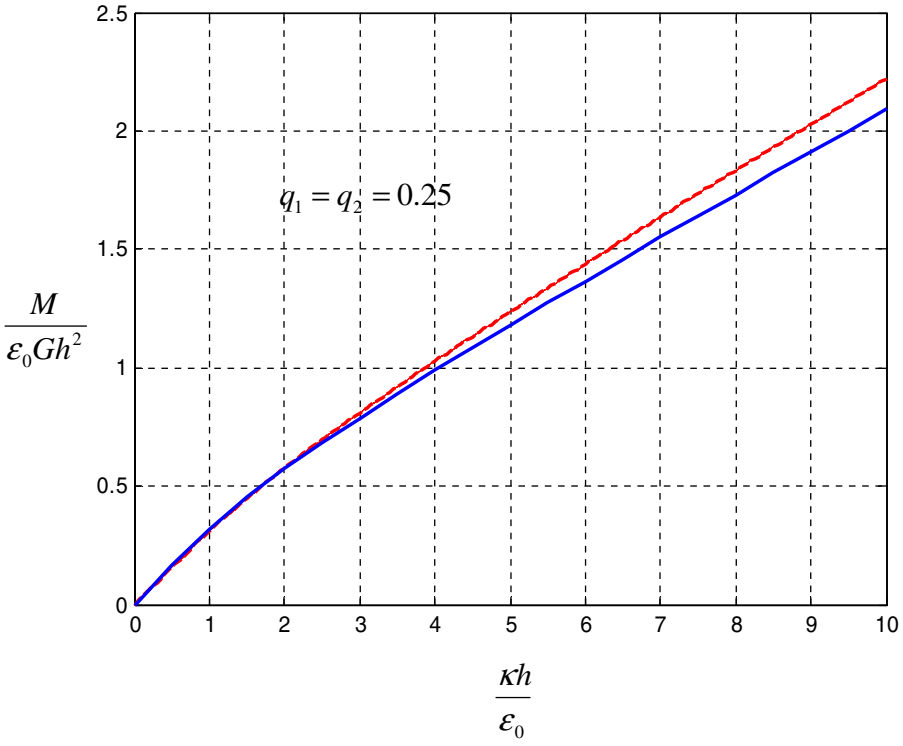

Fig. A5. Beam bending: analytical solution – dashed red line in webversion; 100 1D elements– solid blue line in webversion.

References

Acharya, A., Bassani, J.L., 2000. Incompatibility and crystal plasticity. J. Mech. Phys. Solids 48, 1565–1595.

Acharya, A., Tang, H., Saigal, S., Bassani, J.L., 2004. On boundary conditions and plastic strain-gradient discontinuity in lower-order gradient plasticity. J. Mech. Phys. Solids 52, 1793–1826.

Aifantis, E.C., 1984. On the microstructural origin of certain inelastic models. Trans. ASME J. Eng. Mater. Tech. 106, 326–330.

Aifantis, E.C., 1987. The physics of plastic deformation. Int. J. Plast. 3, 211–247.

Al-Rub, R.K., Voyiadjis, G.Z., 2006. A physically based gradient plasticity theory. Int. J. Plast. 22, 654–684.

Bassani, J.L., 2001. Incompatibility and a simple gradient theory of plasticity. J. Mech. Phys. Solids 49, 1983–1996.

Bazant, Z.P., Belytschko, T., Chang, T.P., 1984. Continuum theory for strain-softening. J. Eng. Mech. 110, 1666–1692.

Begley, M.R., Hutchinson, J.W., 1998. The mechanics of size-dependent indentation. J. Mech. Phys. Solids 46, 2049–2068.

Brinckmann, S., Siegmund, T., Huang, Y., 2006. A dislocation density based strain gradient model. Int. J. Plast. 22, 1784–1797.

de Borst, R., 1993. A generalization of J2 flow theory for polar continua. Comput. Methods Appl. Mech. Eng. 103, 347–362.

de Borst, R., Muhlhaus, H.B., 1992. Gradient-dependent plasticity: formulation and algorithmic aspects. Int. J. Numer. Methods Eng. 35, 521–539.

de Borst, R., Pamin, J., 1996. Some novel developments in finite element procedures for gradient-dependent plasticity. Int. J. Numer. Methods Eng. 39, 2477–2505.

Devincre, B., Kubin, L.P., 1997. Mesoscopic simulations of dislocations and plasticity. Mater. Sci. Eng. A234, 8–14.

Deshpande, V.S., Needleman, A., van der Giessen, E., 2005. Plasticity size effect in tension and compression of single crystals. J. Mech. Phys. Solids 53, 2661–2691.

Fleck, N.A., Hutchinson, J.W., 1993. A phenomenological theory of strain gradient effects in plasticity. J. Mech. Phys. Solids 41, 1825–1857.

Fleck, N.A., Hutchinson, J.W., 1997. Strain gradient plasticity. Adv. Appl. Mech. 33, 296–361.

Fleck, N.A., Hutchinson, J.W., 2001. A reformulation of strain gradient plasticity. J. Mech. Phys. Solids 49, 2245–2271.

Fleck, N.A., Muller, G.M., Ashby, M.F., Hutchinson, J.W., 1994. Strain gradient plasticity: theory and experiment. Acta Metall. Mater. 42, 475–487.

Fredriksson, P., Gudmundson, P., 2005. Size-dependent yield strength of thin films. Int. J. Plast. 21, 1834–1854.

Gao, H., Huang, Y., Nix, W.D., Hutchinson, J.W., 1999. Mechanism-based strain gradient plasticity-I. Theory. J. Mech. Phys. Solids 47, 1239–1263.

Gudmundson, P., 2004. A unified treatment of strain gradient plasticity. J. Mech. Phys. Solids 52, 1379–1406.

Gurtin, M.E., 2000. On the plasticity of single crystals: free energy, microforces, plastic-strain gradients. J. Mech. Phys. Solids 48, 989–1036.

Gurtin, M.E., 2002. A gradient theory of single-crystal viscoplasticity that accounts for geometrically necessary dislocations. J. Mech. Phys. Solids 50, 5–32.

Gurtin, M.E., 2003. A framework for small-deformation viscoplasticity: free energy, microforces, strain gradients. Int. J. Plast. 19, 47–90.

Gurtin, M.E., Anand, L., 2005. A theory of strain-gradient plasticity for isotropic, plastically irrotational materials. Part II: Finite deformations. Int. J. Plast. 21, 2297–2318.

Han, C.S., Gao, H., Huang, Y., Nix, W.D., 2005a. Mechanism-based strain gradient crystal plasticity-I. Theory. J. Mech. Phys. Solids 53, 1188–1203.

Han, C.S., Gao, H., Huang, Y., Nix, W.D., 2005b. Mechanism-based strain gradient crystal plasticity-II. Anal. J. Mech. Phys. Solids 53, 1204–1222.

Han, C.S., Hartmaier, A., Gao, H., Huang, Y., 2006. Discrete dislocation dynamics simulations of surface induced size effects in plasticity. Mater. Sci. Eng. A 415, 225–233.

Han, C.S., Ma, A., Roters, F., Raabe, D., 2007. A finite element approach with patch projection for strain gradient plasticity formulations. Int. J. Plasticity 23, 690–710.

Huang, Y., Gao, H., Nix, W.D., Hutchinson, J.W., 2000. Mechanism-based strain gradient plasticity-II. Anal. J. Mech. Phys. Solids 48, 99–128.

Huang, Y., Qu, S., Hwang, K.C., Li, M., Gao, H., 2004. A conventional theory of mechanism-based strain gradient plasticity. Int. J. Plast. 20, 753–782.

Hwang, K.C., Guo, Y., Jiang, H., Huang, Y., Zhuang, Z., 2004. The finite deformation theory of Taylor-based nonlocal plasticity. Int. J. Plast. 20, 831–839.

Hutchinson, J.W., 2000. Plasticity at the micron scale. Int. J. Solids Struct. 37, 225–238.

Leblond, J.B., Perrin, G., Devaux, J., 1994. Bifurcation effects in ductile metals with damage delocalization. J. Appl. Mech. 61, 236–242.

Liu, B., Huang, Y., Li, M., Hwang, K.C., Liu, C., 2004. A study of the void size based on the Taylor dislocation model. Int. J. Plast. 21, 2107–2122.

di Luzio, G., Bazant, Z.P., 2005. Spectral analysis of localization in nonlocal and over-nonlocal materials with softening plasticity or damage. Int. J. Solids Struct. 42, 6071–6100.

McElhaney, K.W., Vlassak, J.J., Nix, D.W., 1998. Determination of indenter tip geometry and indentation contact are for depth-sensing indentation experiments. J. Mater. Res. 13, 1300–1306.

Muhlhaus, H.B., Aifantis, E.C., 1991. A variational principle for gradient plasticity. Int. J. Solids Struct. 28, 845–857.

Needleman, A., Tvergaard, V., 1998. Dynamic crack growth in a nonlocal progressively cavitating solid. Eur. J. Mech. A/Solids 17, 421–438.

Nix, W.D., Gao, H., 1998. Indentation size effects in crystalline materials: a law for strain gradient plasticity. J. Mech. Phys. Solids 46, 411–425.

Ohashi, T., Kawamukai, M., Zbib, H., 2007. A multiscale approach for modeling scale-dependent yield stress in polycrystalline metals. Int. J. Plasticity 23, 897–914.

Pijaudier-Cabot, G., Bazant, Z.P., 1987. Nonlocal damage theory. J. Eng. Mech. ASCE 113, 1512–1533.

Polizzotto, C., Borino, G., Fuschi, P., 1998. A thermodynamically consistent formulation of nonlocal and gradient plasticity. Mech. Res. Comm. 25, 75–82.

Qu, S., Huang, Y., Pharr, G.M., Hwang, K.C., 2006. The indentation size effect in spherical indentation of iridium: a study via the conventional theory of mechanism-based strain gradient plasticity. Int. J. Plast. 22, 1265–1286.

Stolken, J.S., Evans, A.G., 1998. A microbend test method for measuring the plasticity length scale. Acta Mater. 46, 5109–5115.

Stromberg, L., Ristinmaa, M., 1996. FE-formulation of a nonlocal plasticity theory. Comput. Methods Appl. Mech. Eng. 136, 127–144.

Volokh, K.Y., Hutchinson, J.W., 2002. Are lower order gradient theories of plasticity really lower order? J. Appl. Mech. 69, 862–864.

Wallin, M., Ristinmaaw, M., 2005. Deformation gradient based kinematic hardening model. Int. J. Plast. 21, 2025–2050.

Yun, G., Qin, J., Huang, Y., Hwang, K.C., 2004. A study of lower-order strain gradient plasticity theories by the method of characteristics. Eur. J. Mech. A/Solids 23, 387–394.

Zbib, H.M., Diaz, de la Rubia, T., Bulatov, V., 2002. A multiscale model of plasticity based on discrete dislocation dynamics. Trans. ASME J. Eng. Mater. Technol. 124, 78–87.

Zhang, F., Saha, R., Huang, Y., Nix, W.D., Hwang, K.C., Qu, S., Li, M., 2007. Indentation of a hard film on a soft substrate: strain gradient hardening effects. Int. J. Plast. 23, 25–43.